Downloaded from SAE International by John Schmidt, Tuesday, November 10, 2015

973341

Head/Neck Kinematic Response of Human Subjects in Low-Speed Rear-End Collisions

Gunter P. Siegmund, David J. King, and Jonathan M. Lawrence
MacInnis Engineering Associates

Jeffrey B. Wheeler, John R. Brault, and Terry A. Smith
Biomechanics Research & Consulting, Inc.

Copyright 1997 Society of Automotive Engineers, Inc.

ABSTRACT

Limited data exist which quantify the kinematic response of the human head and cervical spine in low-speed rear-end automobile collisions. The objectives of this study were to quantify human head/neck kinematics and how they vary with vehicle speed change and gender during low-speed rear-end collisions. Forty-two human subjects (21 male, 21 female) were exposed to two rear-end vehicle-to-vehicle impacts (speed changes of 4 kmlh and 8 km/h). Accelerations and displacements of the head and torso were measured using 6 degree-of-freedom accelerometry and sagittal high speed video respectively. Velocity was calculated by integrating the accelerometer data. Kinematic data of the head and C7-T1 joint axis in the global reference frame, and head kinematic data relative to the C7-T1 joint axis are presented. A statistical comparison between peak amplitude and time-to-peak amplitude for thirty-one common peaks in the kinematic response was performed. Peak amplitudes and time-to-peak amplitude varied significantly with collision severity for most response peaks, and varied significantly with gender for about one quarter of the response peaks.

INTRODUCTION

Whiplash-Associated Disorders (WAD) comprised about 61 percent ($590 million) of all injury claims paid by the Insurance Corporation of British Columbia in 1995 [1,2]. In the United States, neck strains and sprains (assumed to be WAD) are the most serious injuries reported by 40 percent of claimants [3]. Despite the magnitude of this phenomenon, the injury mechanisms causing WAD remain unclear. The incomplete understanding of the injury mechanisms is partially the result of limited occupant kinematic data of the head, neck, and torso during low-speed rear-end collisions. Head and torso kinematic data exist for human subjects exposed to frontal collisions [4], and has been used to construct and validate mathematical models [5]. For rear-end collisions, a common source of WAD [6], the data are less complete.

Previous experiments examining the head, neck, and torso kinematics in low-speed rear-end collisions have used cadavers, anthropomorphic test devices (ATD's), and human subjects. Cadavers and current ATD's lack biofidelity in low-speed collisions [7,8]. The complex intersegmental dynamics produced by a low-speed rear-end collision and the potential role of muscle force in whiplash kinematics currently make the use of human subjects the best method of evaluating occupant kinematics at lower collision severities.

Severy et al, exposed a male volunteer to two rear-end impacts in 1950's vintage vehicles not equipped with head restraints [9]. Horizontal head and shoulder accelerations, and head extension determined from film analysis were reported for both collisions and showed the differential kinematic response of the head and shoulders to a rear-end collision. Mertz and Patrick also exposed a single male volunteer to multiple rear-end impacts with the head both supported and unsupported by a head restraint [7]. The subject in these tests was seated in a rigid seat mounted to a laboratory test sled. Bi-axial head accelerations in the superior-inferior and anterior-posterior directions were recorded and resolved to the estimated center of mass of the head. This measurement technique allowed angular acceleration of the head about the medial-lateral axis to be quantified. These authors recognized that head kinematics relative to the torso were important and later proposed response envelopes for the head and neck based on torque at the occipital condyles as a function of head angle relative to the torso [10].

In two separate and more recent studies, McConnell et al, exposed eight male subjects to multiple

Downloaded from SAE International by John Schmidt, Tuesday, November 10, 2015

impacts in 1980's vintage vehicles [11,12]. Based on their data, the authors developed a semi-quantitative description of the occupant kinematic response to a rear-end impact. Linear acceleration at a number of points on the head and angular acceleration and velocity about the medial-lateral axis of the head were reported. Transient symptoms of WAD were produced despite head extension remaining within the range of voluntary motion. Szabo et al, also in two separate studies, exposed seven male and three female subjects to rear-end impacts using 1970's and 1980's vehicles [13,14]. Resultant accelerations at the head's estimated center of mass were reported for both series of tests and the acceleration at the base of the cervical spine was reported for the first series of five subjects. Szabo et al, found that the peak head acceleration observed in their data was a result of head contact with the head restraint and was not necessarily an indicator of neck injury potential.

Matsushita et al, subjected 22 males and 4 females to sled tests simulating rear-end collisions [15]. Head acceleration in the posterior-anterior direction of the head and bi-axial chest accelerations were reported for numerous pre-impact postures. These authors also used cineradiography to quantify segmental motion of the cervical vertebrae and found that initial posture influenced the kinematic response.

Epidemiological studies have found that women suffer whiplash more frequently than men [16-21]. Most proposed explanations for gender differences are based on observations that females have a greater head mass for their neck area [22] or neck strength [23] than do males. Although WAD have been reported after various impact directions and severities, they occur most commonly after rear-end collisions [6,21,24], and overall injury risk in rear-end collisions generally increases with collision speed change [17].

Although these experimental studies have quantified some of the kinematic response, a detailed volunteer study with .adequate sample size and instrumentation to compare and quantify the absolute and relative motion of the head and torso has yet to be performed. This paper presents detailed kinematic response data for 42 human subjects exposed to low-speed rear-end collisions at two severities, and specifically examines the effect of gender and collision severity on the peak kinematic response of the head, neck, and torso.

MATERIALS AND METHODS

SUBJECTS - Human subject protection policies and procedures were reviewed and approved by the Western Institutional Review Board of Olympia, Washington, USA. A more detailed description of the human subject handling procedures has been published elsewhere [25].

Subjects between 20 and 40 years old were recruited by newspaper and job-line advertisements. Potential subjects were screened by telephone for height and weight (10 - 90th percentile) [26]. Subjects with a history of specific medical conditions or a prior or active injury claim were excluded. Potential subjects were then invited to the lab to undergo an initial screening process. Each subject was seated in an exemplar test seat to ensure that their head and not their neck contacted the head restraint. This criterion eliminated subjects with an erect seated height of 96 cm or greater (the median seated height for a 90th percentile male [27]), and excluded subjects with above-average seated heights who would otherwise have qualified based on standing height. After obtaining informed consent, subjects underwent a cervical magnetic resonance scan. Subjects with a disc bulge greater than 2 mm or degenerative findings deemed moderate or greater by a radiologist were excluded from the study.

Table 1. Mean and standard deviation (SD) of subject age and selected anthropometry.

	Male	Female
N	21	21
Age - yr	26.4 (4.5)	27.1 (4.8)
Age range	21-37	20-40
Height - cm	175.4 (5.2)	164.3 (5.2)
Mass - kg	74.9 (9.7)	62.3 (8.8)
Head Circumference - cm	57.8 (2.2)	55.5 (1.7)

Forty-two subjects (21 males and 21 females) successfully completed the interview, screening, and informed consent and participated in the test procedure. Table 1 contains subject age and selected anthropometry data.

INSTRUMENTATION - Head acceleration was measured using a nine accelerometer array (Kistler 8302B20S1; ±20g, Amherst, NY) arranged in a 3-2-2-2 configuration [28]. A uni-axial angular rate sensor (ATA Sensors ARS-04E; ±100 rad/s, Albuquerque, NM) was attached to the accelerometer unit and oriented along the medial-lateral axis. This redundant sensor was used as a check on the primary head acceleration sensors. The accelerometer arrangement was secured to the subject's head with two straps as shown in Figure 1. The mass of the complete head instrumentation package was 198 grams, including straps and 40 cm of cable. Torso acceleration was measured using a ' tri-axial accelerometer (Summit 34103A; ±7.5g, Akron, OH) and an angular rate sensor (ATA-Sensors DynaCube; ±100 rad/s). Both torso transducers were fastened to an aluminum plate, which was applied in the mid-sagittal plane to the chest immediately below the manubrium with adhesive. Straps over the shoulders and under the arms also secured the plate. The mass of the torso instrumentation package was 255 grams.

The location and orientation of the head and torso instrumentation was measured relative to anatomical landmarks using a three-dimensional digitizer (FaroArm B08-02, Lake Mary, FL) with single-point accuracy of k0.30 mm [29]. The accuracy of the

Downloaded from SAE International by John Schmidt, Tuesday, November 10, 2015

Figure 1. Head Instrumentation

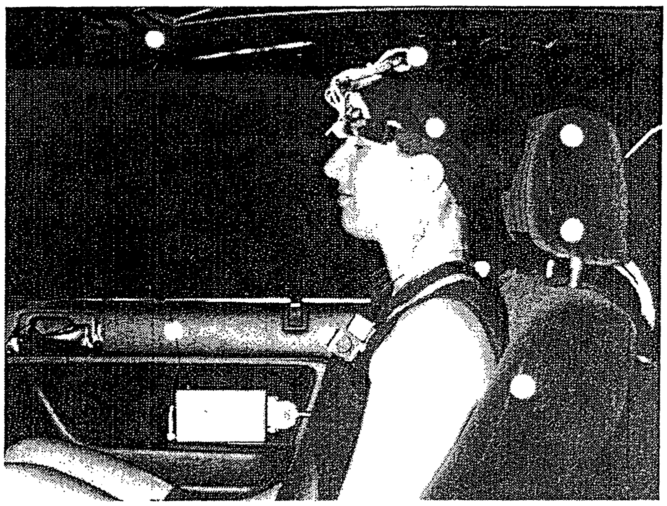

Figure 2. Subject seated in the vehicle

FaroArm was certified according to the manufacturer's instruction before every test.

Vehicle Instrumentation - Vehicle speeds were measured with a 5th wheel (MEA 5th Wheel, Richmond, BC) attached to each vehicle. Uni-axial load cells (Sensotec Model 41; range ±45 000 N, Columbus, OH) inserted at both rear bumper mounts of the Honda recorded the longitudinal component of the impact force (lateral and vertical components were assumed to be negligible). Bumper contact onset and duration were detected with two ribbon switches (Nortel TapeSwitch 121BP; 2 N activation force, Scarborough, ON) connected in parallel and applied to the rear bumper of the target vehicle. Head restraint contact was detected by three force sensitive resistors (Interlink Electronics Inc.; 0.2 N activation, Camarillo, CA) connected in parallel and applied to the front of the head restraint.

High-Speed Videography - Digital video of sagittal plane motion relative to earth was captured using an OmniSpeed HS motion capture system (Speed Vision Technologies, Solana Beach, CA) and high-speed camera (JCLabs 250; 512 x 216 lines resolution, Mountain View, CA). Video data were recorded at 250 frames per second (fps) using a shutter speed of 1/1000 s. Reflective targets were applied to the subject, seat, and vehicle (see Figure 2). Vehicle and seat targets were 25 mm in diameter and subject targets were 20 mm in diameter. Head targets were applied over the glabella, left temporomandibular joint, left lateral aspect of the cranium, and to the left side of the head accelerometer assembly; torso targets were applied in the mid-sagittal plane to the chest accelerometry and over the spinous process of the seventh cervical vertebrae (C7); seat targets were applied to the upper seat back and head restraint; and vehicle targets were applied to the interior surfaces of the right front door and upper door frame (roof rail).

Digital video data were digitized using OmniSpeed AutoTracker software with a combined experimental setup and video system accuracy of ± 2 mm at the vertical plane containing the seat centerline. Additionally, stationary video cameras (30 fps) were used to record front, overhead, and overall views of each test and an onboard video camera mounted to the driver's A-pillar captured an oblique view.

TEST PROCEDURE - With their head stabilized in an optometrist's forehead rest, anatomical landmarks (glabella, upper incisors, vertex, opisthocranion, occiput, external acoustic meati, and bilateral lower rims of the orbits) were measured in three-dimensions with the FaroArm for each subject. Head and torso accelerometry and video targets were applied and their locations measured relative to the previously-measured landmarks. These data were subsequently referenced to the Frankfort plane, defined by the digitized locations of the lower orbit rims and the external acoustic meati. The torso instrumentation and head video targets were also digitized relative to selected vehicle and seat locations with the subject seated in the vehicle. The torso accelerometry was referenced to the mid-sagittal plane, manubrium and C7 spinous process. The right acromioclavicular joint, greater trochanter, and lateral femoral epicondyle were also digitized to record the subject's seated posture.

The subjects were seated and restrained by a lap and shoulder seat belt in the front passenger seat of the test vehicle. Subjects were instructed to sit normally in the seat, face forward with their head level, place their hands on their lap, and to relax prior to impact.

Because of the potential effect of pre-impact neck muscle contraction on kinematics, special attention was devoted to depriving the subjects of visual and aural cues of the impending impact and to ensuring subjects

Downloaded from SAE International by John Schmidt, Tuesday, November 10, 2015

were relaxed before the impact. A black felt curtain separated the target vehicle from the bullet vehicle and instrumentation equipment to eliminate visual cues. Foam ear plugs and music were used to defeat aural cues. No test personnel were visible to the subject in the minutes preceding the impact. The relaxed state of the occupant was confirmed visually with a live video feed from the A-pillar camera and by monitoring EMG signals from the sternocleidomastoid and cervical para-spinal muscles bilaterally for at least one-minute prior to impact.

An aligned collision between a rolling bullet vehicle and a stationary target vehicle was used for this study. Both vehicles were in neutral and their engines were not running. The bullet vehicle accelerated down a ramp and its front bumper squarely struck the rear bumper of the unbraked target vehicle. After impact, the target vehicle rolled into gravel located 3 meters ahead of the vehicle and was decelerated to rest at about 0.12 g.

Subjects were exposed to two impacts, one which produced a 4 km/h speed change on the target vehicle and another which produced an 8 km/h speed change. The order of impact-severity presentation was randomized. In all cases, the two impacts were separated by at least seven symptom-free days.

VEHICLE SPECIFICATIONS - The bullet vehicle was a 1981 Volvo 240DL station wagon (mass 1618 kg) and the target vehicle was a 1990 Honda Accord LX 4-door sedan (mass 1414 kg). The bullet vehicle was unaltered. The target vehicle's windshield, left doors, left B-pillar, driver's seat, and rear bench seat were removed. A hole was cut in the roof over the test subject to allow overhead filming. A custom B-pillar installed midway between the actual B- and C-pillar locations compensated for the reduced stiffness resulting from removal of the actual B-pillar. Mass was added to the vehicle to offset the removed parts. No damage (other than minor plastic straining of the Honda's rear bumper cover) was sustained by either vehicle over the 100-plus pre-study and study impacts.

Aside from minor modifications to accommodate seat instrumentation, the Honda's seat remained in its stock condition. The fore/aft seat adjustment was locked in the full rear position and the seat back angle was maintained at about 27 degrees from the vertical. The head restraint was adjusted and locked to the full-up position for all subjects. Detailed information regarding seat back modifications made to accommodate the head restraint instrumentation has been presented elsewhere [30].

DATA ACQUISITION - Accelerometer, angular rate sensor, load cell and contact switch data were acquired at 10 kHz and each data channel conformed to SAE J211, Channel Class 1000 [31]. Signal conditioners onboard the vehicle were tethered to four 16-channel, 12-bit, simultaneous-sample-and-hold Win30 DAQ cards (United Electronics Incorporated, Watertown, MA). Low-pass line-noise filters were inserted immediately before the DAQ boards. All four DAQ boards were installed in the same computer and driven by a single external clock. Two seconds of data were acquired for each test, with a minimum of 0.4 s of pre-impact data. Fifth wheel data were acquired at 128 Hz and triggered by the bumper contact switch. Fifth wheel data were recorded simultaneously for both vehicles for 1 s before and 4 s after impact. A synchronization signal from the high-speed video camera was recorded by the DAQ system and LED's indicating bumper and head restraint contact were placed in each camera's field of view.

REFERENCE FRAMES - Kinematic parameters obtained from the occupant-mounted transducers were initially resolved to local head and torso reference frames. For analysis and presentation, these data were resolved to the global reference frame at the appropriate origin. The head and neck origins, and the direction of the global axes, were defined as follows (Figure 3):

The origin of the head was located at the estimated location of the head's center of mass, assumed to lie in the mid-sagittal plane. Its superior-inferior and anterior-posterior position was estimated for each subject based on regression equations published by Clauser et al [32]. The origin of the neck was located in the mid-sagittal plane at the C7-T1 joint axis (center of rotation of the base of the neck), estimated to be at the midpoint between the C7 spinous process and the manubrium [33].

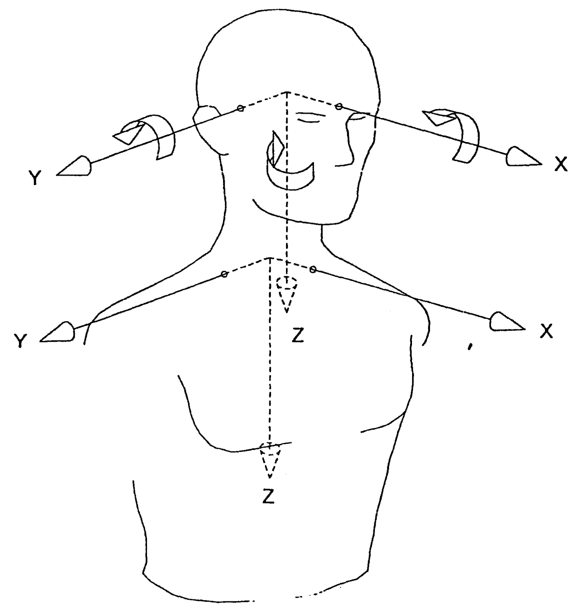

Figure 3. Reference frames for the head and C7-T1 joint axis. The broad arrows show the direction of positive rotation about each axis. (adapted from reference 34).

The z-axis of the global reference frame was defined parallel to the direction of the earth's gravity and positive down. The x-axis was defined such that the xz-plane was parallel to the longitudinal axis of the vehicle and was defined positive toward the front of the vehicle. The y-axis was positive to the right. The global origin was arbitrary, but for reporting purposes, it was assumed to be at the pre-impact origin of either the head or C7-T1

Downloaded from SAE International by John Schmidt, Tuesday, November 10, 2015

joint axis, whichever was appropriate. Flexion and extension of the headlneck and torso in the sagittal plane occurred about the y-axis, with extension defined positive and flexion negative.

DATA PROCESSING - The kinematic parameters extracted from the data were the linear and angular acceleration, velocity and position of the head center of mass and the C7-T1 joint axis. Since the instrumentation was mounted externally, the kinematic parameters were measured externally and then resolved to the estimated internal location of the head center of mass and the C7-T1 joint axis assuming rigid body kinematics. The treatment of each group of data is outlined below:

Head Kinematics - The head accelerometers were sensitive to DC and therefore the I g field from the earth's gravity was subtracted from the data in order to yield the transient linear accelerations due to the impact. To determine the initial component of the I g field on each channel, the mean signal of each accelerometer over the 100 ms preceding impact was assumed to be due to gravity. Because the 3-2-2-2 configuration yielded three independent measures of the three orthogonal components (in the 3-2-2-2 reference frame) making up the I g field, the magnitude and direction of the 1g field were estimated from these redundant data by minimizing the sum of squares error. The resulting vector estimate of the 1g field defined the initial orientation of the head relative to the lab reference frame. An additional assumption that the x-axis of the head frame lay in the xz-plane of the global frame was required to obtain a unique rotation matrix between the two reference frames.

During and after the collision, the head frame translated and rotated relative to the lab frame. The time-varying three-dimensional orientation angle between the two frames was computed by first integrating the angular acceleration (a) to obtain the angular velocity (ω), and then using the orientation vector technique to update the transformation matrix between the body-fixed and inertial reference frames [35]. Because head and torso rotation were predominantly in the xz-plane, the orientation vector method produced a transformation matrix that was essentially identical to a direct double integration of the angular acceleration vector, or a method of Euler rates and angles [36].

The angular acceleration (a) required for the foregoing calculation was computed using Equation I [28]. The instantaneous angular acceleration thus obtained was independent of the instantaneous angular velocity, which minimized accumulated errors and yielded an estimate of the angular acceleration which remained reliable for a longer duration than other methods [28]. Angular velocity of the head about the medial-lateral axis was compared with the uni-axial angular rate sensor on the head, and sagittal head angle was compared with the sagittal high speed video for agreement.

$$\alpha_x = \frac{a_{z1} - a_{z0}}{2\rho_{y1}} - \frac{a_{y3} - a_{y0}}{2\rho_{z3}}$$
$$\alpha_y = \frac{a_{x3} - a_{x0}}{2\rho_{z3}} - \frac{a_{z2} - a_{z0}}{2\rho_{x2}} \quad (1)$$
$$\alpha_z = \frac{a_{y2} - a_{y0}}{2\rho_{x2}} - \frac{a_{x1} - a_{x0}}{2\rho_{y1}}$$

where α_i = angular acceleration along axis i,
a_i = acceleration at accelerometer i,
ρ_i = distance between accelerometers.

The origin of the 3-2-2-2 assembly, could not be placed at the head center of mass of a human subject. Therefore, the head acceleration computed at the origin of the 3-2-2-2 assembly was resolved to the center of gravity of the head using Equation 2 [37].

$$a = \mathbf{a}_A + \alpha \times \mathbf{r}_{B/A} + \omega \times (\omega \times \mathbf{r}_{B/A}) \quad (2)$$

where a = acceleration at point B,
a = acceleration at point A,
a = angular acceleration
ω = angular velocity, and
$\mathbf{r}_{B/A}$ = position vector between points A and B

Torso Kinematics - The tri-axial linear accelerometer used to measure chest acceleration was sensitive to DC and was also corrected for the uniform I g field of the earth's gravity. Unlike the head assembly correction, redundant channels were not available. The mean of each axis of the linear accelerometer over the 100 ms preceding impact was assumed to define the initial direction of the I g field. This assumption, combined with the assumption that the x-axis of the chest accelerometry assembly was contained in the xz-plane of the global reference frame, was used to determine the rotation matrix between the initial sensor reference frame and the global frame. Torso rotation angles were computed as described earlier and used to update the rotation matrix during impact-induced motion.

Unlike the head accelerometer assembly, the rotational kinematics of the torso were directly measured using a tri-axial angular rate sensor. The angular rate sensor data contained substantially more noise than the linear accelerometer data and were therefore optimally filtered [38,39] before computation. Digital low-pass filters based on the data of five subjects were used to filter the angular velocity data of all subjects. After filtering, the angular acceleration was computed from the angular velocity by calculating the slope between the instantaneous angular velocity 10 ms before and after the time of interest. Intervals shorter than 10 ms produced unrealistically short, high angular acceleration peaks. Because the contribution of the $(a \times \mathbf{r})$ term in

Downloaded from SAE International by John Schmidt, Tuesday, November 10, 2015

Equation 2 to the acceleration at the C7-T1 joint axis was small, the differentiation process was not refined.

The sensitive axes of the tri-axial linear accelerometer used for measuring the torso acceleration did not pass through a single point. Although torso transducer rotation was not large, the accelerations of the y- and z-axes were corrected to a single point on the sensitive x-axis using equation 2. This correction was typically less than 10 percent of the peak signal, but was performed because the internal offset of the sensitive axes was large (about 15 mm) relative to the distance from the sensor origin to the C7-T1 joint axis (typically about 90 mm). Linear accelerations at the C7-T1 joint axis were then calculated from the measured torso transducer signals in the same manner as for the head.

High Speed Video Data - Reflective target data extracted from the high-speed video were first corrected for camera lens barrel distortion using a 5th order polynomial (odd terms only) [40]. The polynomial coefficients were determined using a 10 cm by 10 cm grid covering the camera's field of view (about 0.90 m by 1.20 m at the centerline of the target vehicle's seat), and then minimizing the sum of squares error between the actual and digitized grid. Because the camera-to-subject distance was relatively short (5 m), the data for targets located off the mid-sagittal plane were also adjusted for parallax [40]. The camera axis was assumed to be perpendicular to the plane of vehicle and occupant motion. Since a target could not be positioned a priori over the origins of the head and torso reference frames, the path of these points was calculated assuming a fixed position relative to the actual markers.

Collision severity - Vehicle position data from the 5th wheels were differentiated across a 16 ms window, and speed change was then determined from scale plots of vehicle speed versus time [41]. The bumper load-cell sensor bias, estimated as the mean signal over the 100 ms preceding impact, was removed from the data before summing the left and right load cells to obtain total collision force. The sum was then integrated and divided by the vehicle mass to confirm vehicle speed change.

Some parameters were measured using multiple methods to confirm the response. For instance, head angle about the y-axis was computed from the 3-2-2-2 accelerometers and the uni-axial angular rate sensor, and then compared to the high-speed video data. The acceleration data presented in this paper were computed from the accelerometer and angular rate sensors, and the position and angle data were extracted from the high speed video. Velocity data were computed by integrating acceleration rather than differentiating displacement data because of the inherent random-noise-reducing effect of the integration process.

STATISTICAL ANALYSIS - Gender and speed change were the primary variables in this study. The null hypotheses were that neither gender nor speed change affected the kinematic response of an occupant exposed to a low-speed, rear-end collision.

Peak amplitude and time-to-peak amplitude were extracted for peaks common to the absolute and relative linear and angular acceleration, velocity and position data of the head and C7-T1 of each subject. The effect of gender and speed change on the amplitude and time of each common peak in the kinematic response was tested using a single analysis of variance (ANOVA) for each of the two extracted measures. The covariance of peak amplitude and time-to-peak amplitude was examined to ensure that single tests were valid. A method of unweighted means was used to account for the unequal samples in each cell of the ANOVA [42].

To ensure the probability of a false positive was less than 0.05 across the 31 peaks examined, a Bonferroni adjustment was used [43]. Each of the 62 ANOVA tests (31 peak amplitudes and 31 time-to-peak amplitudes) was required to achieve a significance level of 0.0008 (0.05162) to be judged significantly related to speed change or gender.

RESULTS

Forty-two subjects were exposed to impacts. Three subjects withdrew between their 4 kmlh and 8 km/h tests, and all subjects who underwent the 8 km/h test first completed the study. Impacts at the 4 and 8 km/h level were repeatably produced (Table 2).

Position and angle data obtained from high speed video were acquired for all subjects (Table 3a). Because of the nature of the accelerometer calculations, a failure of one transducer rendered the test data incomplete. Incomplete data were collected for six tests, which reduced the number of subjects for whom complete transducer data were recorded (Table 3b). The full data set was used to calculate the position-based

Table 2. Vehicle speed and collision properties at the 4 and 8 km/h level. All properties were significantly different at the two levels.

Property	4 km/h level	8 kmlh level
Volvo impact speed (km/h)	4.86 (0.12)	10.02 (0.06)
Honda speed change (5th wheel)	3.95 (0.11)	8.10 (0.11)
(load cell)	4.04 (0.09)	8.07 (0.07)
Restitution	0.59 (0.01)	0.56 (0.01)
Collision duration (ms)	138 (4)	135 (2)
Time of peak force (ms)	42 (2)	35 (1)
Peak bumper force (kN)	27.0 (0.9)	48.5 (0.5)

Tables 3a and 3b. Number of tests used for the analysis of (a) position and angle from high speed video (left), and (b) acceleration and velocity from transducer data (right).

	Male	Female	Total
4 km/h	21	21	42
8 km/h	20	19	39
Total	41	40	81

	Male	Female	Total
4 km/h	19	20	39
8 km/h	19	17	36
Total	38	37	**75**

Downloaded from SAE International by John Schmidt, Tuesday, November 10, 2015

results, whereas the reduced data set was used to calculate the acceleration and velocity results presented here.

Only sagittal plane motion was considered in this analysis, which yielded 27 kinematic response signals: nine signals (a_x, a_z, v_x, v_z, s_x, s_z, α_y, ω_y, θ_y) each for the absolute motion of the head, absolute motion of the C7-T1, and relative motion of the head with respect to C7-T1. Motion out of the sagittal plane, i.e., translational motion along the y-axis and rotational motion about the x and z axes, were small and varied considerably between subjects. The complete sagittal kinematic response data of all subjects is attached in Appendix A.

Good agreement between double-integrated accelerometer data and high-speed video position data was achieved for the kinematic response of the head and the translational components of the C7-T1 joint axis (Figure 4). Integrated angle data from the uni-axial angular rate sensor (ARS) on the head also compared well with the accelerometer and video data. Differences between accelerometer and high-speed-video data for the angle (θ) of the C7-T1 joint axis relative to the earth were likely caused by skin motion and/or filtering. Extraneous vertical motion of the torso transducers was visible in the video; however, manually digitized check measurements of the manubrium showed that the automatically-tracked video target data reliably measured upper torso angle. Skin motion was also present in the head data of some subjects, however to a much lesser degree than in the torso data.

In all tests, initial flexion between the head and the torso was observed. Although only slight flexion was present in some subjects, maximum flexion of 13 degrees from the initial orientation of the head relative to the C7-T1 joint axis was reached by some subjects.

Relative horizontal motion between the head and C7-T1 joint axis also occurred in all subjects. Forward acceleration of the C7-T1 origin typically began about 25 to 35 ms after impact, coincident with vertical acceleration of the head relative to the earth. Forward horizontal acceleration and angular acceleration of the head relative to the earth began about 10 to 30 ms after the onset of vertical head acceleration. Observable positive C7-T1 joint axis rotation relative to the earth began about 30 to 40 ms after impact and forward horizontal displacement began about 20 ms later. Positive head rotation relative to the earth was detected about 50 to 70 ms after impact, after 1 to 5 degrees of flexion between the head and C7-T1 joint axis had developed from torso motion.

Forward horizontal head displacement with respect to the earth was not observed until about 80 to 110 ms after impact. By this time, between 1 to 5 cm of rearward horizontal translation had developed between the head center of mass and the C7-T1 origin. Maximum rearward horizontal translation of the head's center of mass relative to the C7-T1 origin varied between 2.5 and 11 cm.

Head restraint contact was made in 80 of 81 tests. Excluding one male at the 4 km/h level who did not contact the head restraint, the mean time from bumper contact to head restraint contact was 118 ± 18 ms at the 4 km/h level and 94 ± 13 ms at the 8 km/h level. The duration of head restraint contact was 95 ± 17 ms at the 4 km/h level and 103 ± 13 ms at the 8 km/h level.

At head restraint contact, the head was rotating rearward and just beginning to translate forward in the global reference frame. Relative to the C7-T1 joint axis, however, head restraint contact was made with the head in its initially flexed and retracted position. Rearward rotation (extension) of the head relative to the C7-T1 joint axis did not begin until after head restraint contact, and in about 20 percent of the tests, the head never extended rearward of its original orientation relative to the C7-T1 joint axis.

Peak horizontal head acceleration relative to the earth occurred during head restraint contact for all subjects who contacted the head restraint. Peak horizontal head speed relative to the earth averaged about 1.9 times the target vehicle speed change across all subjects and both speed changes. The peak horizontal speed of the C7-T1 joint axis relative to the earth averaged about 1.6 times the vehicle speed change.

Thirty-one response peaks common to all subjects were analyzed for the effect of speed change and gender on peak kinematic response (Figure 5). Some kinematic response signals contained multiple peaks common to all subjects, whereas other signals were excluded from the analysis because of dissimilar subject response. At the adjusted significance level of 0.0008, the amplitude of 28 peaks and the time of 27 peaks varied significantly with vehicle speed change (Tables 4a and 4b). The amplitude of seven peaks and the time to eight peaks varied significantly with gender. The interaction term was not significant for the amplitude or time of any of the selected peaks.

DISCUSSION

The number of subjects in this study allowed statistical comparisons to be made between the kinematic response of male and female subjects at the two selected speed changes in rear-end automobile collisions. The larger peak amplitudes demonstrated at the 8 km/h level compared to the 4 km/h level for most of the kinematic parameters tested provides insight into the effect of collision severity on the kinematic response of human subjects in low-speed rear-end collisions. However, the importance of the absolute values of each peak and the relationship of each kinematic parameter to the injury mechanism causing WAD has not yet been established.

When addressing the potential for injury, the kinematics of the head relative to the C7-T1 joint axis may be more important than simple peak values of the head or C7-T1 joint axis relative to the earth. For

Downloaded from SAE International by John Schmidt, Tuesday, November 10, 2015

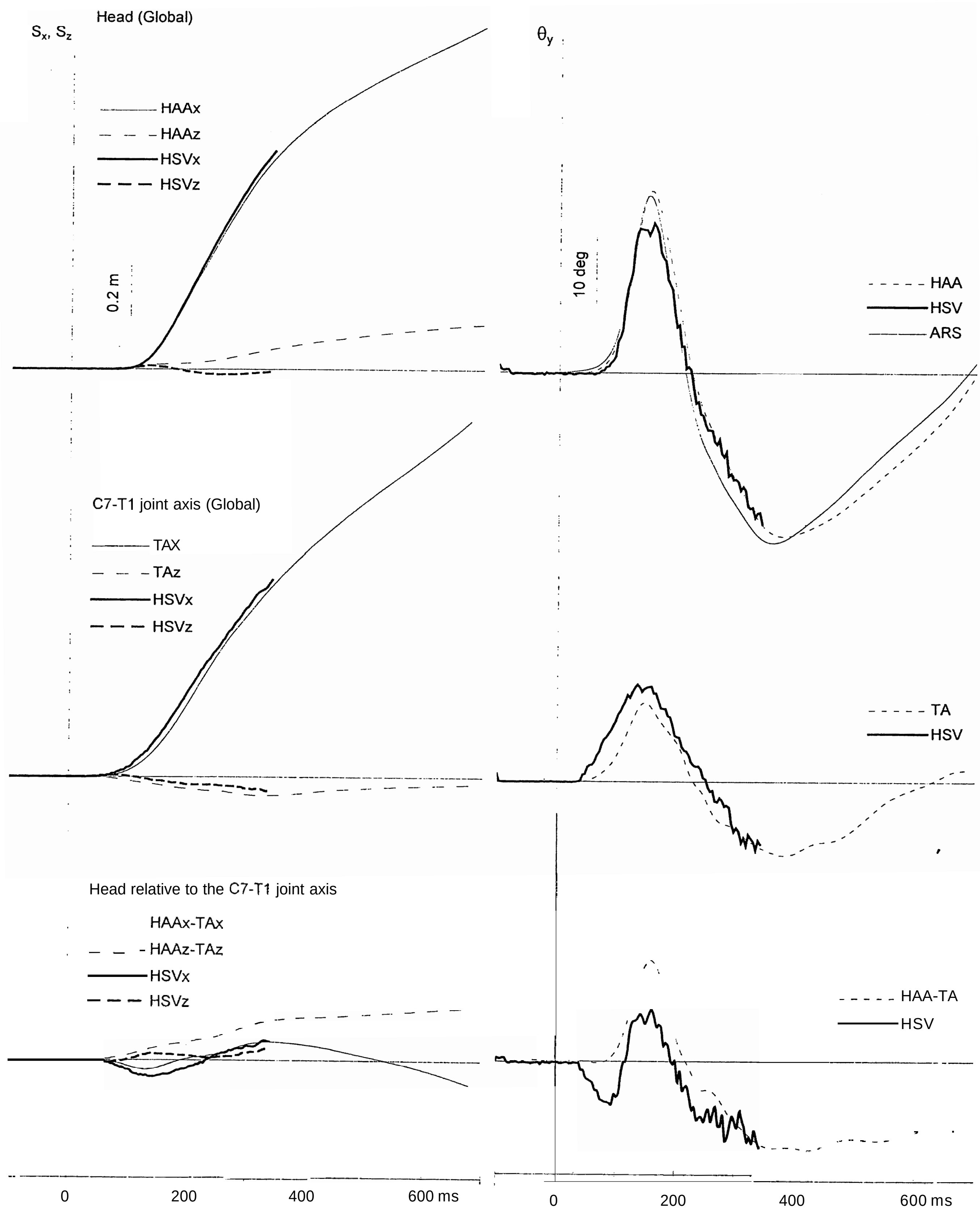

Figure 4 Typical agreement between the double-integrated accelerometery and high-speed video position (s_x,s_z) and angle (θ_y) data for the head (top row) and C7-T1 joint axis (middle row) in the global reference frame, and the head relative to the C7-T1 origin (bottom row). Abbreviations are as follows: HAA - Head accelerometer array. TA - torso accelerometers, HSV - high speed video.

Downloaded from SAE International by John Schmidt, Tuesday, November 10, 2015

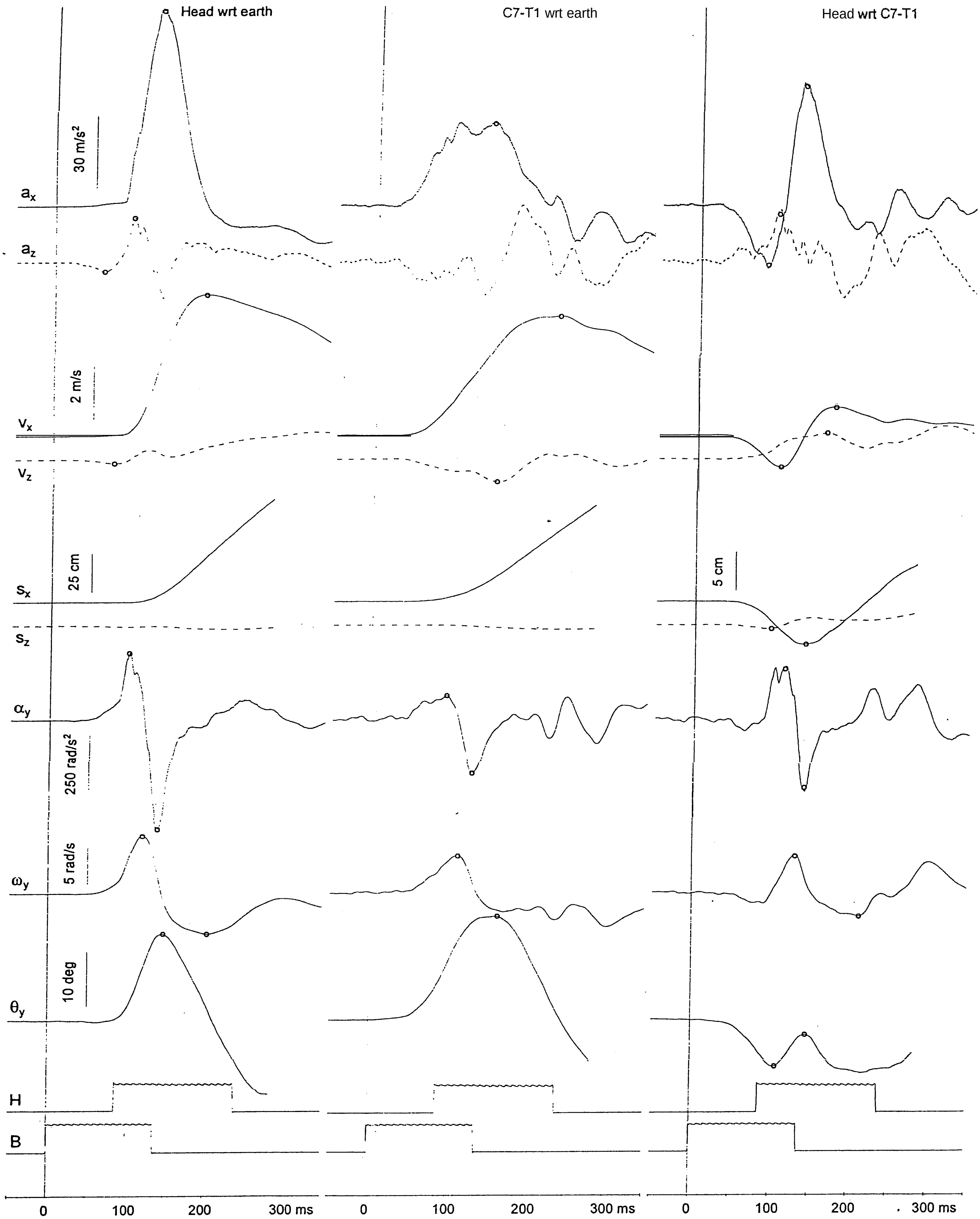

Figure 5. Exemplar kinematic response data for a female at the 8km/h level. The three graphs depict (left) the head response relative to earth, (center) the C7-T1 joint axis relative to earth, and (right) the head relative to the C7-T1 joint axis. H and B data depict head restraint contact and bumper contact respectively. Circles identify peaks used for analysis. Note scale change for s_x and s_y of the head relative to C7-TI joint axis.

Downloaded from SAE International by John Schmidt, Tuesday, November 10, 2015

Table 4a. Mean, standard deviation (SD), and ANOVA results for amplitudes of selected peaks in the kinematic response data.

Kinematic Parameter†			Units	8 km/h Female	8 km/h Male	4 km/h Female	4 km/h Male	P-Values Gender	Severity	Interaction
Head	a	+	m/s²	91.3(11.4)	84.0(12.5)	38.9(5.7)	29.3(6.2)	0.0002*	0.0000'	0.5955
	a_z	-		-3.8(2.1)	-3.3(2.6)	-2.9(1.1)	-2.3(1.0)	0.2140	0.0398	0.8988
		+		22.4(6.0)	16.9(5.2)	11.0(2.6)	8.5(2.3)	0.0001*	0.0000'	0.1438
	v_x	+	m/s	4.38(0.15)	4.27(0.18)	2.20(0.17)	1.96(0.22)	0.0002*	0.0000'	0.1251
	v_z	-		-0.13(0.07)	-0.11(0.10)	-0.10(0.05)	-0.08(0.05)	0.3092	0.1989	0.9435
	a,	+	rad/s²	293(67)	319(74)	152(45)	140(37)	0.5869	0.0000*	0.1721
				-673(193)	-737(201)	-319(103)	-268(80)	0.8546	0.0000'	0.1066
	ω_y	+	rad/s	9.26(2.66)	10.79(2.33)	5.17(1.42)	5.43(1.05)	0.0512	0.0000*	0.1638
				-7.11(1.38)	-7.78(1.44)	-4.88(1.06)	-4.71(0.80)	0.3654	0.0000"	0.1349
	θ_y	+	deg	15.89(4.83)	23.81(5.02)	13.42(4.57)	17.26(3.73)	0.0000*	0.0000*	0.0505
C7-T1	a	+	mls²	42.8(5.8)	36.3(6.5)	20.8(3.0)	17.9(2.4)	0.0001*	0.0000*	0.1034
	v_x	+	m/s	3.79(0.16)	3.57(0.24)	1.76(0.28)	1.56(0.21)	0.0003*	0.0000'	0.8381
	v_z	-		-0.65(0.15)	-0.61(0.15)	-0.36(0.05)	-0.38(0.08)	0.5851	0.0000*	0.3275
	a,	+	radls²	113(27)	102(46)	56(19)	50(1 5)	0.2158	0.0000*	0.6789
				-292(87)	-206(92)	-115(46)	-88(52)	0.0011	0.0000*	0.0804
	ω_y	+	rad/s	4.16(0.90)	3.80(0.99)	2.06(0.54)	2.02(0.76)	0.2799	0.0000*	0.4072
	θ_y	+	deg	16.83(2.58)	17.67(2.43)	10.28(1.56)	11.36(2.55)	0.0695	0.0000*	0.8209
Head w.r.t. C7-T1	a	-	rn/s²	-25.3(3.6)	-26.0(5.1)	-15.1(3.4)	-13.4(1.8)	0.5487	0.0000*	0.1664
		+		57.9(12.1)	59.9(15.2)	28.8(4.9)	26.4(6.2)	0.9466	0.0000*	0.3624
	a	+		28.1(6.1)	25.1(8.5)	13.9(5.0)	12.1(3.4)	0.0826	0.0000*	0.6731
	v_x	-	m/s	-0.94(0.21)	-1.14(0.18)	-0.67(0.13)	-0.71(0.09)	0.0026	0.0000*	0.0474
		+		0.84(0.14)	0.95(0.11)	0.61(0.14)	0.56(0.16)	0.3836	0.0000*	0.0169
	v_z	+		1.03(0.15)	0.90(0.21)	0.56(0.11)	0.51(0.09)	0.0127	0.0000*	0.2162
	s_x	-	m	-0.056(0.013)	-0.072(0.016)	-0.043(0.010)	-0.050(0.009)	0.0001*	0.0000*	0.1393
	s_z	-		-0.006(0.002)	-0.005(0.001)	-0.004(0.002)	-0.003(0.001)	0.0378	0.0001*	0.9730
	a	+	radls²	353(168)	391(133)	165(75)	149(64)	0.6834	0.0000*	0.3219
				-549(250)	-678(231)	-276(131)	-243(101)	0.2698	0.0000*	0.0653
	ω_y	+	rad/s	8.18(3.90)	10.18(2.89)	4.41(1.84)	4.29(1.55)	0.1296	0.0000*	0.0885
				-5.39(1.44)	-7.40(1.70)	-4.40(1.66)	-4.73(1.47)	0.0021	0.0000*	0.0244
	θ_y	-	deg	-7.73(2.41)	-6.58(3.12)	-3.70(1.46)	-2.66(1.38)	0.0306	0.0000*	0.9114
		+		-0.41(3.86)	6.69(5.34)	3.56(4.56)	6.39(3.59)	0.0000*	0.0681	0.0345

† symbol "+" refers to a positive peak in the lab reference frame directions, "-" refers to a negative peak
* statistically significant

Table 4b. Mean, standard deviation (SD), and ANOVA results for time (milliseconds) to selected peaks in the kinematic response data.

Kinematic Parameter'			8 kmlh Female	8 kmlh Male	4 km/h Female	4 kmlh Male	P-Values Gender	Severity	Interaction
Head	a	+	128(7)	140(6)	150(10)	161 (9)	0.0000*	0.0000*	0.8575
	a_z	-	64 (5)	67 (7)	81 (4)	83 (6)	0.0855	0.0000*	0.7162
		+	108(8)	112(9)	133 (9)	137 (10)	0.1137	0.0000*	0.8362
	v_x	+	201 (13)	202(10)	222 (18)	231 (25)	0.3156	0.0000'	0.3579
	v_z	-	80 (7)	80(10)	99 (6)	101 (7)	0.6699	0.0000*	0.5680
	α_y		108(7)	114(10)	125 (9)	128 (13)	0.0633	0.0000*	0.5478
			144(7)	156(12)	168 (13)	178 (13)	0.0003*	0.0000'	0.7959
	ω_y	+	126(8)	135(8)	145 (10)	147 (10)	0.0096	0.0000*	0.1124
		-	184(15)	206(13)	218 (19)	226 (17)	0.0003*	0.0000*	0.0778
	θ_y	+	143 (7)	154 (9)	171 (13)	178 (13)	0.0008*	0.0000*	0.5615
C7-T1	a_x	+	128 (12)	119 (17)	110 (11)	117 (10)	0.7103	0.0015	0.0199
	v_x	+	228 (25)	226 (22)	233 (33)	251 (30)	0.2449	0.0277	0.1240
	v_z	-	138 (18)	135 (14)	139 (20)	139 (14)	0.7687	0.5357	0.7265
	α_y	+	86 (13)	88 (15)	109 (15)	106 (18)	0.8106	0.0000*	0.4880
		-	131 (9)	135 (11)	156 (18)	162 (23)	0.1915	0.0000*	0.7763
	ω_y	+	111 (8)	112 (12)	127 (15)	130 (21)	0.5513	0.0000*	0.7678
	θ_y	+	140(10)	158(17)	168(12)	189(22)	0.0000'	0.0000'	0.5621
Head w.r.t. C7-T1	a	-	86 (9)	93(11)	103(9)	105(10)	0.0695	0.0000*	0.2239
		+	129 (9)	141 (6)	151 (12)	161 (11)	0.0000*	0.0000*	0.5187
	a_z	+	117 (12)	112 (11)	127 (16)	133 (11)	0.9288	0.0000*	0.0663
	v_x	-	105 (7)	114 (8)	124 (7)	130 (8)	0.0001*	0.0000*	0.4628
		+	178 (22)	190 (11)	219 (30)	221 (24)	0.1975	0.0000*	0.3496
	v_z	+	139 (11)	135 (10)	154 (15)	152 (9)	0.2557	0.0000*	0.6639
	s_x	-	135 (11)	150 (9)	162 (15)	171 (15)	0.0002*	0.0000*	0.2984
	s_z	-	89 (12)	88 (12)	107 (11)	100 (18)	0.2398	0.0000*	0.3394
	α_y	+	117 (10)	118 (9)	126 (13)	132 (13)	0.2455	0.0001*	0.4268
		-	148 (7)	155 (9)	170 (13)	179 (17)	0.0086	0.0000*	0.6453
	ω_y	+	132 (8)	139 (9)	148 (14)	149 (10)	0.1215	0.0000*	0.2829
		-	191 (20)	205 (19)	215 (18)	222 (19)	0.0275	0.0000*	0.4441
	θ_y	-	102 (7)	102 (10)	116 (9)	106 (16)	0.0735	0.0013	0.0722
		+	148(10)	158(9)	175(17)	181 (15)	0.0108	0.0000*	0.4704

† symbol "+" refers to a positive peak in the lab reference frame directions, "-" refers to a negative peak
* statistically significant

Downloaded from SAE International by John Schmidt, Tuesday, November 10, 2015

instance, female subjects had greater horizontal accelerations of the head and C7-T1 relative to the earth than male subjects, but this difference was not present for the head relative to the C7-T1 joint axis. This finding underscores the potential for misinterpretation of results referenced only to the global reference frame.

The greater and earlier peak horizontal acceleration of the head and C7-T1 joint axis (relative to the earth) of the female subjects and the larger and later peak head extension of the male subjects were consistent with the larger body mass and head size (and therefore head mass) of the male subjects and the correspondingly lower frequency response of the seat back/occupant system. Both seat back stiffness and occupant mass govern the frequency response of the seat back, and variations in seat back stiffness have been shown to amplify or attenuate differential motion between the head and neck [44]. Greater male peak head extension may also be related to a lower relative head restraint position for the male subjects than for the female subjects.

The reason for the gender differences found for other response peaks is less clear. A regression analysis which incorporates anthropometry, seated posture, and head restraint adjustment may yield insight into the parameters responsible for the gender differences observed in this study.

Differences in the horizontal distance between the back of the head and the front of the head restraint, known as "backset", have been shown to affect head neck motion using a Hybrid III dummy equipped with a RID neck [44]. Backsets greater than 10 cm have correlated with increased neck symptom duration [45], and lower vertical head restraint position has correlated with an increased incidence of neck injuries in rear-end collisions [46]. Because the adjusted seat back angle and head restraint position relative to the seat in the present study were fixed, inter-subject differences in anthropometry and posture resulted in variable horizontal and vertical head restraint positions. For all subjects, however, the top of the head restraint was above the ears and backset was less than 10 cm. Both head restraint backset and vertical position were potential confounding variables in this study and warrant additional investigation.

In an observational study of the motoring public, 15 percent of observed drivers had backsets less than 10 cm, and only 10 percent of drivers had a combination of backset less than 10 cm and top of the head restraint adjusted above the ears [47]. The subjects in the current study therefore represent the small segment of the motoring public with "optimal" head restraint protection.

The observed initial flexion between the head and torso was a result of torso rotation preceding head rotation: torso rotation began about 30 to 40 ms after impact, whereas head rotation was not observed until about 50 to 70 ms after impact. The position and angle of the head and the position of the upper torso initially remained stationary relative to the earth, while the pelvis and lower torso were accelerated forward by the seat

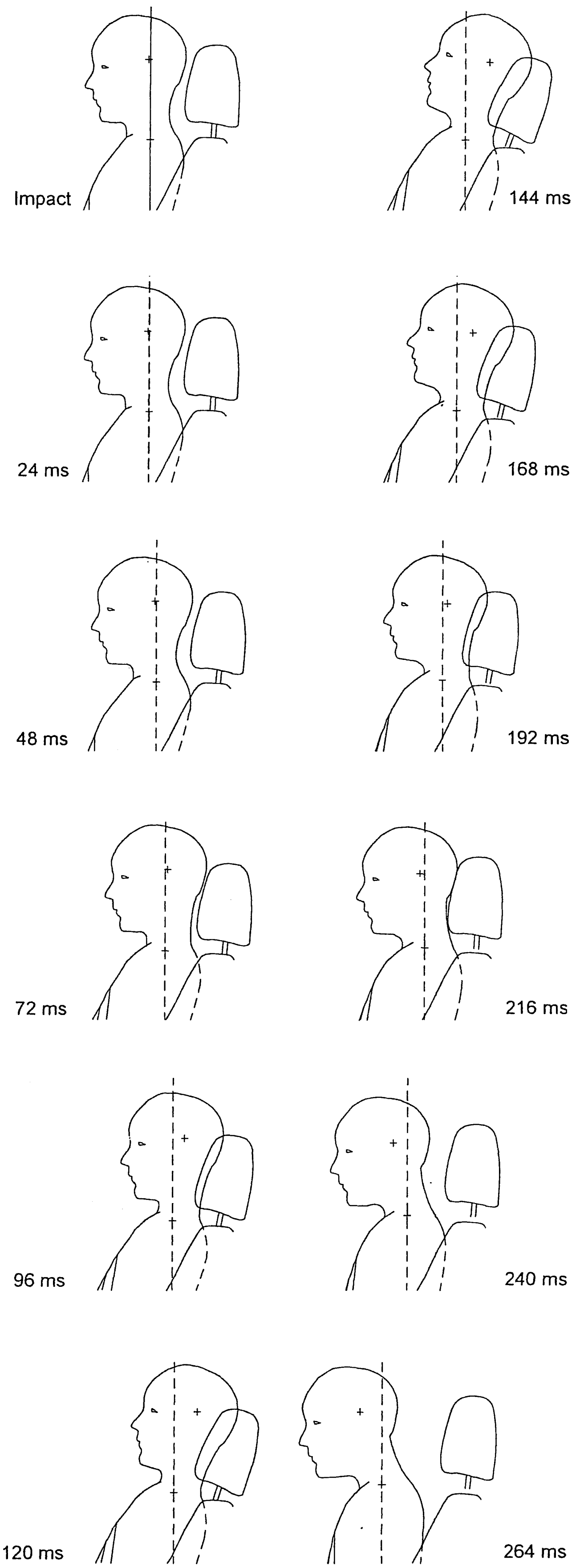

Figure 6. Exemplar kinematic response of the head and C7-T1 joint axis in 24 ms steps after initial contact for an 8 km/h speed change. Note the horizontal position of the head COG (+) in relation to the initial position (solid line) and instantaneous position (dashed line) of the C7-T1 joint axis.

Downloaded from SAE International by John Schmidt, Tuesday, November 10, 2015

Table 5. Comparison of peak kinematic parameters reported in previous research (rear-end collisions only)

Parameter	Units	Severy et al. [9][a]	Mertz et al. [7][b]	McConnell et al.[11,12]	Szabo et al.[13,14]	Matsushita et al.[15]	Siegmund et al	
Number of human subjects		1 M	1 M	8 M[c]	7 M, 3 F[c]	16 M, 3 F	21M, 21F	20M, 19F
Number of tests		2	2	24	17	19	42	39
Collision speed change	(km/h)	8.4, 9.5[d]	13.5, 14.3[e]	3.5 - 10.9	8 - 10	2.5 - 5.0	4	8
Test type		vehicle	sled	vehicle	vehicle	sled	vehicle	vehicle
Peak head acceleration	(g)	5.0. 2.9'	- 7[g]	3 - 6'	6.6 - 16.6[g]	2.7 - 6.3[h]	1.6 -5.0'	6.7 - 12.0'
Peak head angular acceleration (-y dir.)	(radls^2)		- 200	400 - 600[i]			160-510	450-1260
Peak head angular velocity (-y direction)	(rad/s)			16 - 20[i]			2.4 - 7.3	5.4 - 17.7
Peak head extension from initial position	(deg)	34, 38	37	< - 60	7 - 30		4 - 27	9 - 33
Peak acceleration at top of torso	(g)				4.5 - 7.4[k]	1.6 - 2.9[k]	1.4 - 2.6'	2.7 - 5.9'

a. subject aware of second Impact
b kinematic data for only one impact reported, subject tense and aware, no head restraint
c data drawn from two test series
d computed by integrating acceleration data
e sled impact speed, rebound assumed to be zero
f. horizontal acceleration relative to the earth
g resultant acceleration
h. acceleration in the anterior-posterior direction of the head
i data from high-speed video
k direction in global coordinates not known

back. This forward motion of the pelvis and lower torso set up a positive rotation of the torso about the y-axis and resulted in flexion between the stationary head and rotating torso.

Rearward horizontal translation of the head relative to the C7-T1 joint axis was prominent in all subjects (Figure 6) and was greater in male subjects than female subjects. A comparison between the amount of rearward horizontal translation of the head center of mass relative to the C7-T1 joint axis and the active range of motion in retraction of the subjects in this study (3.1 ± 0.9 cm [25]) suggests that dynamic retraction may have approached or exceeded the subjects' active range of motion. Although some of the rearward horizontal translation between the head's center of mass and C7-T1 origin was the result of head extension relative to the C7-T1 joint axis, rearward horizontal translation occurred in all subjects whereas relative head extension did not. In subjects whose head remained flexed during the entire impact, horizontal translation between the top of the cervical spine (base of the skull) and the C7-T1 origin may have been larger than indicated by the horizontal translation between the head center of mass and the C7-T1 joint axis. It has been previously reported that small amounts of horizontal translation between the head and C7-T1 bring the craniovertebral junction into maximal flexion and that translation of the head relative to the torso may cause damage at the craniovertebral junction [48]. Additional work is needed to determine whether dynamic retraction of the top of the cervical column relative to the C7-T1 origin exceeded active range of motion, and whether this translation was related to symptom production.

Previous research has reported that the head of some test subjects never reached anatomical extension relative to the torso (extension beyond the head/torso orientation when standing upright) [13]. The current data showed that the head of some subjects never rotated rearward of its initial "anatomically flexed" position relative to the C7-T1 joint axis. Additional work is required to determine whether this pattern of motion was associated with symptom production, and whether the flexed position of the head relative to the C7-T1 joint axis at head restraint contact contributed to a WAD injury mechanism.

Peak head extension relative to C7-T1 was less than 20 degrees from the initial flexed position of the head relative to the torso for all subjects. Active neck range of motion in extension for the subjects in this study was 70 ± 8 degrees from the anatomical neutral position [25]. None of the subjects exceeded their extension range of motion. This finding indicates that hyperextension of the neck was not the mechanism responsible for transient symptoms produced in this study [25], and is consistent with other studies producing transient symptoms without hyperextension [11,12,13].

The torso and head over-speed observed in the current data appear to be larger than that qualitatively reported in a previous human subject study [12]. Torso over-speed was previously described as slightly greater than the vehicle's post-impact speed and head over-speed was described as slightly greater than torso speed. Over-speed is likely a function of seat back elasticity and frequency response, and differences in seat back properties between studies may account for the greater over-speed found in the current data.

The statistical findings of this research cannot be compared directly to the results of previous kinematic investigations into low-speed rear-end collisions because no previous studies examined gender and collision severity effects, largely due to small test populations. A general comparison between peak kinematic parameters observed in this study and those reported in the literature was possible (Table 5). This comparison was restricted largely to the kinematic response of the head relative to the earth except for two studies [14,15] that reported acceleration measured at the approximate location of the C7 spinous process and on the frontal surface of the chest respectively.

Peak head acceleration varied widely between the studies in Table 5, perhaps due to differences between pre-impact muscle contraction, collision

Downloaded from SAE International by John Schmidt, Tuesday, November 10, 2015

severity, seat backs and head restraints. Angular acceleration of the head relative to the earth was higher in the current study, however the data from other studies presented in Table 5 were calculated from high speed film rather than accelerometers. Higher peak head angular velocity and greater head extension in the data of McConnell et al, [12] may be related to a higher head position relative to the head restraint used in their tests. Head extension compared favorably with data reported by Szabo et al, [13,14] who used a head restraint height similar to that used in the present study. Peak acceleration at the base of the cervical spine also compared well with the limited previous data [14,15], although the comparison may not be valid because the data were not measured at or resolved to the same points.

This study examined the sagittal plane response of the head and torso of ideally seated occupants with a well-adjusted head restraint in an aligned vehicle collision within a single vehicle and seat position. Additional studies are needed to quantify the effect on the kinematic response of the many variables controlled in the present study.

SUMMARY

Head and torso kinematic response data for 21 male and 21 female subjects exposed to a controlled series of low-speed rear-end automobile collisions have been presented. Initial flexion between the head and torso was observed in all subjects. Retraction of the head center of mass relative to the C7-T1 joint axis was present in all subjects, whereas extension of the head relative to its initial position with respect to the C7-T1 joint axis was not present in all subjects.

Significant gender differences existed between the peak amplitude and time-to-peak amplitude for about one quarter of the thirty-one common peaks in the kinematic response data. Significant differences between the two collision severities were demonstrated for both the amplitude and time of most common peaks in the kinematic response data.

ACKNOWLEDGMENTS

This study is part of a larger study examining the kinematic, kinetic, and muscle responses, and clinical outcome of subjects exposed to low-speed rear-end automobile collisions. This study was partially funded by a grant awarded under the Technology BC program administered by the Science Council of British Columbia. Remaining funding was provided by MacInnis Engineering Associates and Biomechanics Research & Consulting, Inc.

The authors wish to thank Elaine Brault, Ian Brault, Jamie Catania, Brad Heinrichs, and Jeff Nickel for their valuable contributions, and the staff at MacInnis Engineering Associates and Biomechanics Research & Consulting, Inc for their assistance and patience.

REFERENCES

1 Quebec Task Force on Whiplash-Associated Disorders. Whiplash associated disorders (WAD), Redefining "whiplash" and its management. Quebec City, QC: Societe de I'assurance automobile du Quebec, January 1995.

2. Fockler SKF, Vavrik J & Kristiansen. Educating drivers to correctly adjust head restraints: Assessing the effectiveness of three different interventions. 39th Annual Proceedings of the Association for the Advancement of Automotive Medicine, pp. 95-109. Des Plaines, OH: Association for the Advancement of Automotive Medicine, 1996.

3. Insurance Research Council. Auto Injuries: Claiming behavior and its impact on insurance costs. Oak Brook, IL, 1994.

4. Thunnissen J, Wismans J, Ewing CL & Thomas DJ. Human volunteer head-neck response in frontal flexion: A new analysis (952721). 39th Stapp Car Crash Conference Proceedings (P-299), pp. 439-460. Warrendale, PA: Society of Automotive Engineers, 1995.

5 de Jager M, Sauren A, Thunnissen J & Wisman J. A global and a detailed mathematical model for head-neck dynamics (962430). 40th Stapp Car Crash Conference Proceedings (P-305), pp. 269-281. Warrendale, PA: Society of Automotive Engineers, 1996.

6 Sturzenegger M, DiStefano G, Radanov BP & Schnidrig A. Presenting symptoms and signs after whiplash injury: The influence of accident mechanisms. Neurology 1994; **44:** 688-693.

7 Mertz HJ & Patrick LM. Investigation of the kinematics and kinetics of whiplash (670919). Proceedings of the 11th Stapp Conference, pp. 175-206. Warrendale PA: Society of Automotive Engineers, 1967.

8. Scott MW, McConnell WE, Guzman HM, et al. Comparison of human and ATD head kinematics during low-speed rearend impacts (930094). Warrendale PA: Society of Automotive Engineers, 1993.

9. Severy DM, Mathewson JH & Bechtol CO. Controlled automobile rear-end collisions, an investigation of related engineering and medical phenomena. Canadian Services Medical Journal, pp. 727-759, November, 1955.

10. Mertz HJ & Patrick LM. Strength and response of the human neck (710855). 15th Stapp Car Crash Conference Proceedings, pp. 207-255. Warrendale, PA: Society of Automotive Engineers, 1971.

McConnell WE, Howard RP, Guzman HM, et al. Analysis of human test subject kinematic responses

Downloaded from SAE International by John Schmidt, Tuesday, November 10, 2015

to low velocity rear end impacts (930889). Warrendale, PA: Society of Automotive Engineers, 1993.

12. McConnell WE, Howard RP, Van Poppel J, et al. Human head and neck kinematics after low velocity rear-end impacts - Understanding "whiplash" (952724). 39th Stapp Car Crash Conference Proceedings (P-299), pp. 215-238. Warrendale, PA: Society of Automotive Engineers, 1995.

13. Szabo TJ, Welcher JB, Anderson RD, et al. Human occupant kinematic response to low speed rear-end impacts (940532). In: Backaitis S, ed. Occupant Containment and Methods of Assessing Occupant Protection in the Crash Environment *(SP-1045)*, pp. 23-36. Warrendale, PA: Society of Automotive Engineers, 1994.

14. Szabo TJ & Welcher JB. Human subject kinematics and electromyographic activity during low speed rear impacts (962432). 40th Stapp Car Crash Conference (P-305), pp. 295-315. Warrendale, PA: Society of Automotive Engineers, 1996.

15. Matsushita T, Sato TB, Hirabayashi K, et al. X-ray study of the human neck motion due to head inertia loading (942208). Warrendale, PA: Society of Automotive Engineers, 1994.

16. O'Neill B, Haddon W, Kelley AB & Sorenson WW. Automobile head restraints - Frequency of neck injury in relation to the presence of head restraints. American Journal of Public Health, March 1972, pp 399-406.

17. Kahane CJ. An evaluation of head restraints - Federal motor vehicle safety standard 202 (DOT HS-806 108). Washington DC: US Department of Transportation, National Highway Traffic Safety Administration, February 1982.

18. Lovsund P, Nygren A, Salen B & Tingvall C. Neck injuries in rear end collisions among front and rear seat occupants. Proceedings of 1988 International IRCOBI Conference on the Biomechanics of Impact, pp.319-325. Bron, France: IRCOBI Secretariat, 1988.

19. Kihlberg JK. Flexion-torsion neck injury in rear impacts. Proceedings of the Thirteenth Annual Conference of the American Association for Automotive Medicine, pp. 1-16. Des Plaines, OH: American Association for Automotive Medicine, 1969.

20. Balla JI. The late whiplash syndrome. Aust. N.Z. J. Surg. 1980; **50**:6 p.610-614.

21. Otremski I, Marsh JL, Wilde BR, McLardy Smith PD & Newman RJ. Soft tissue cervical spinal injuries in motor vehicle accidents. Injury 1989; **20:** 349-351.

22. States J, Balcerak J, Williams J, et al. Injury frequency and head restraint effectiveness in rear-end impacts (720967). Warrendale PA: Society of Automotive Engineers, 1972.

23. Snyder RG, Chaffin DB & Foust DR. Bioengineering study of basic physical measurements related to susceptibility to cervical hyperextension-hyperflexion injury (UM-HSRI-BI-75-6). Ann Arbor, MI: University of Michigan, Highway Safety Research Institute, September, 1975.

24. Olney DB & Marsden AK. The effect of head restraint and seat belts on the incidence of neck injury in car accidents. Injury 1986; **17:** 365-367.

25. Brault JR, Wheeler JB, Siegmund GP, Brault EJ. Clinical response of human subjects to rear-end automobile collisions (in press). Archives of Physical Medicine and Rehabilitation.

26. Najjar MF & Rowland M. Anthropometric Reference Data and Prevalence of Overweight, United States, 1976-80, Data from the National Health Survey series 11, No. 238 (PHS) 87-1688. Hyattsville MD: National Center for Health Statistics, Department of Health and Human Services, October 1987.

27. Diffrient N, Tilley AR & Bardagiy JC. Humanscale Manual. The MIT Press,' Cambridge, MA, 1974.

28. Padgaokar AJ, Krieger KW & King AI. Measurement of angular acceleration of a rigid body using linear accelerometers (No. 75-APMB-3). Transactions of the American Society of Mechanical Engineers, pp 522-526, September 1975.

29. Faro Technologies Inc. FaroArm Bronze Series User's Manual. Lake Mary, FL, 1995.

30. Lawrence JM, Siegmund GP & Nickel JS. Measuring head restraint force and point of application during low-speed rear-end automobile collisions (970397). In: Irwin A & Backaitis S, ed. Occupant Protection and Injury Assessment in the Automotive Crash Environment *(SP-1231)*, pp. 225-37. Warrendale, PA: Society of Automotive Engineers, 1997.

31. Society of Automotive Engineers. SAE recommended practice: Instrumentation for impact tests (SAE J211 Jun 88). 1989 SAE Handbook, Volume 4, On-highway vehicles and off-highway machinery, pp. 34.184 - 34.191. Warrendale, PA: Society of Automotive Engineers, 1989.

32. Clauser CE, McConville JT & Young JW. Weight, volume, and center of mass of segments of the human body (AMRL-TR-69-70). Yellow Springs, OH: Wright Patterson Air Force Base, Aerospace Medical Research Laboratory, August 1969.

Queisser F, Bluthner R & Seidel H. Control of positioning the cervical spine and its application to

Downloaded from SAE International by John Schmidt, Tuesday, November 10, 2015

measuring extensor strength. Clinical Biomechanics 1994; **9:** 157-161, May.

34. Backaitis SH & Mertz HJ (Eds). Hybrid III: The first human-like crash test dummy (PT-44). Warrendale, PA: Society of Automotive Engineers, 1994.

35. Mital NK & King AI. Computation of rigid-body rotation in three-dimensional space from body fixed linear accelerometer measurements. Journal of Applied Mechanics 1979; **46:** 925-930, December.

36. Mital HK. Computation of rigid-body rotation in 3D space from body-fixed acceleration measurements. Ph.D. Dissertation, Detroit MI: Wayne State University, 1978.

37. Beer FP & Johnston ER. Vector mechanics for engineers, Statics and dynamics (3rd edition). McGraw Hill, 1978.

38. Rabiner LR & Gold B. Theory and application of digital signal processing. Prentice Hall, Englewood Cliffs NJ, 1975.

39. Press WH, Teukolsky SA, Vetterling WT & Flannery BP. Numerical recipes in C, The art of scientific computing (2nd Edition). Cambridge University Press, 1992.

40. Moffit FH & Mikhail EM. Photogrammetry, Third Edition. New York, NY: Harper & Row Publishers, 1980.

41. Siegmund GP, King DJ & Montgomery DT. Using barrier impact data to determine the speed change in aligned, low-speed vehicle-to-vehicle collisions (960887). Accident reconstruction: Technology and animation VI (SP-1150), pp. 147-167. Warrendale, PA: Society of Automotive Engineers, 1996.

42. Kleinbaum DG & Kupper LL. Applied regression analysis and other multivariable methods. Duxbury Press, Boston, MA, 1978.

43. Devore JL. Probability and Statistics for Engineering and the Sciences. Brooks/Cole Publishing Company, Monterey, CA, 1982.

44. Svensson MY, Lovsund P, Haland Y & Larsson S. The influence of seat-back and head-restraint properties on the head-neck motion during rear-impact. Accid. Anal. and Prev. 28: 221-227, 1996.

45. Olsson I, Bunketorp O, Carlsson G, Gustafsson C, Planath I, Norin H & Ysander L. An in-depth study of neck injuries in rear-end collisions. Proceedings of 1990 International IRCOBI Conference on the Biomechanics of Impact. Bron, France: IRCOBI Secretariat, 1990.

46. Nygren A, Gustafsson H & Tingvall C. Effects of different types of headrests in rear-end collisions. 10th Experimental Safety Vehicle Conference, p. 85-90. Washington, DC: National Highway Traffic Safety Administration, US DOT, 1985.

47. Viano DC & Gargan MF. Headrest position during normal driving: Implications to neck injury risks in rear crashes. 39th Annual Proceedings of the Association for the Advancement of Automotive Medicine, pp. 215-229. Des Plaines, OH: Association for the Advancement of Automotive Medicine, 1995.

48. Penning L. Acceleration injury of the cervical spine by hypertranslation of the head, Part I, Effect of normal translation of the head on cervical spine motion: A radiology study. European Spine Journal 1992, **1**: 7-12.

Downloaded from SAE International by John Schmidt, Tuesday, November 10, 2015

Appendix A - Summary of the absolute and relative kinematic response data for the head and C7-T1 joint axis.

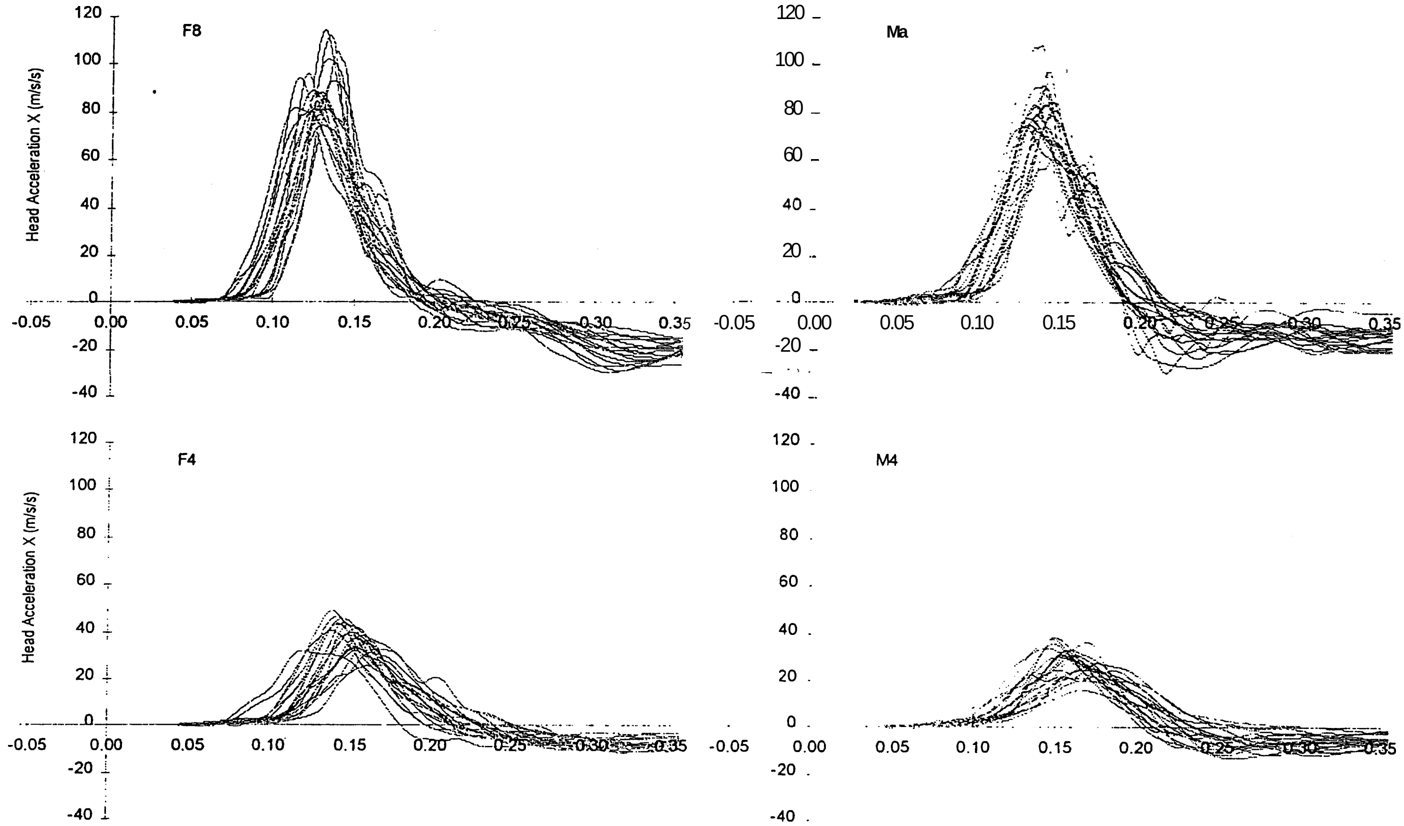

Figure A1. Head acceleration (m/s^2) in the x-direction as a function of time (s). F = female. M = male. **4** = **4** krnlh level, 8 = 8 km/h level.

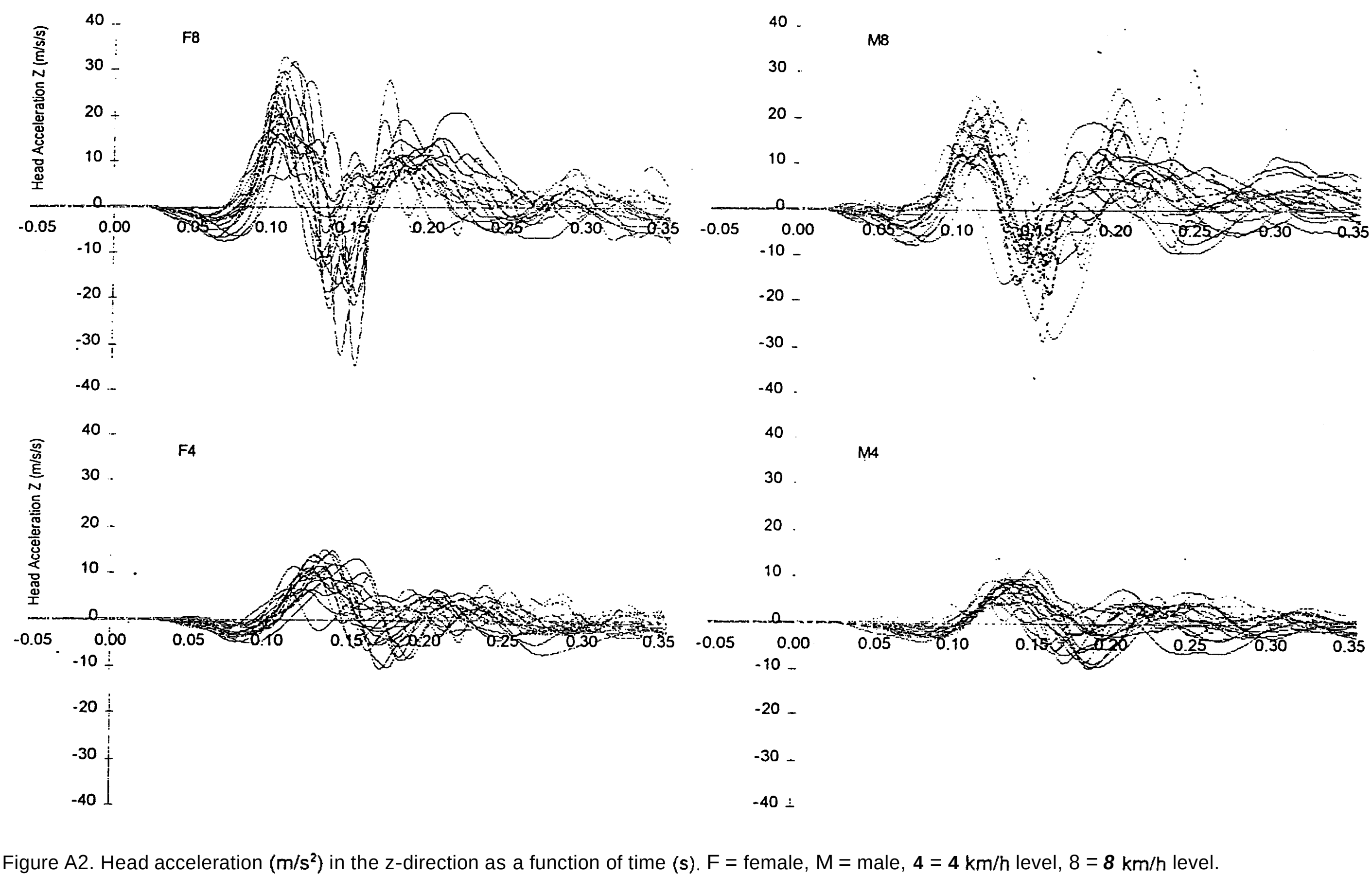

Figure A2. Head acceleration (m/s^2) in the z-direction as a function of time (s). F = female, M = male, **4** = **4** km/h level, 8 = ***8*** km/h level.

Downloaded from SAE International by John Schmidt, Tuesday, November 10, 2015

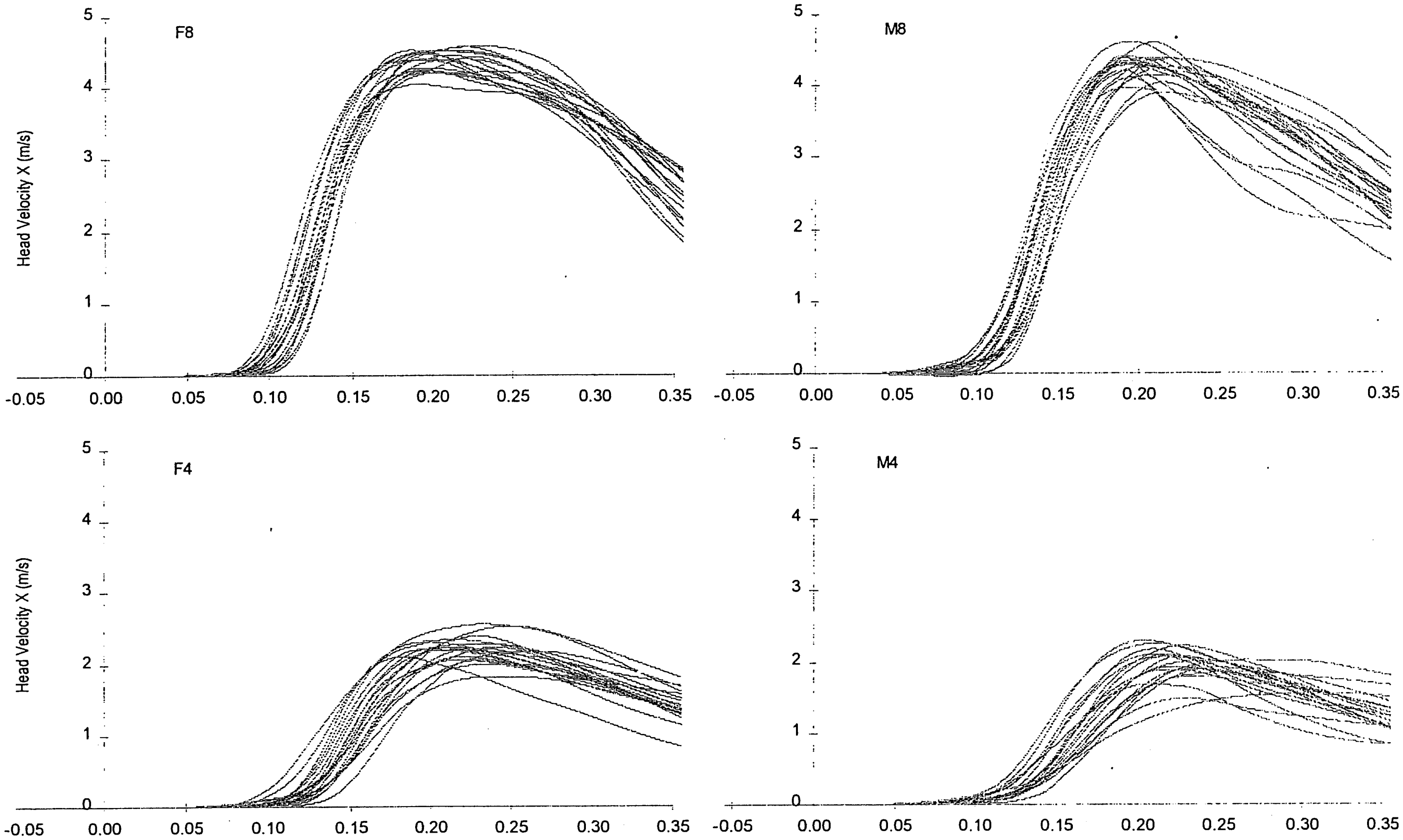

Figure A3. Head velocity (m/s) in the x-direction as a function of time (s). F = female, M = male, 4 = 4 kmlh level, 8 = 8 kmlh level

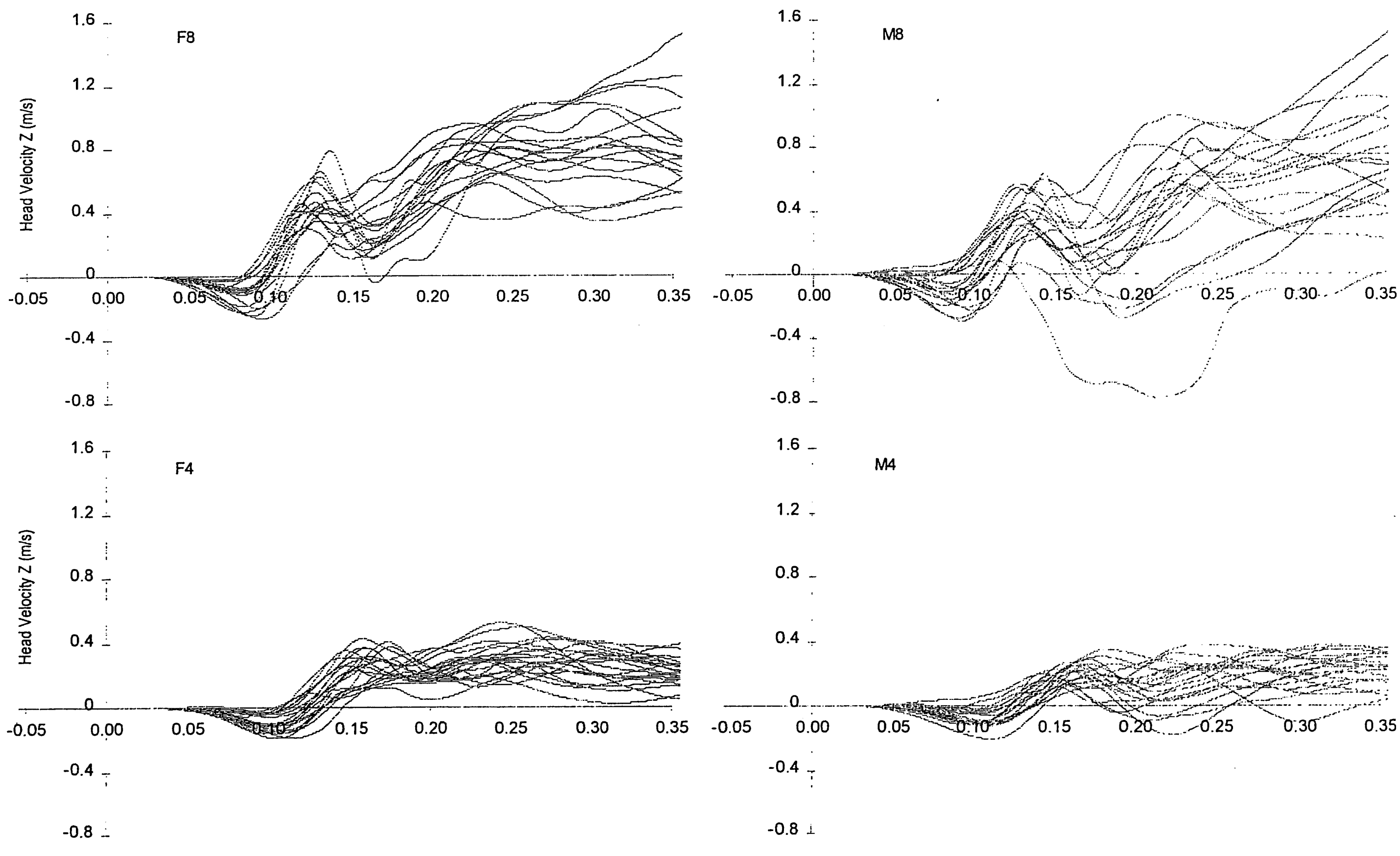

Figure A4. Head velocity (m/s) in the z-direction as a function of time (s). F = female, M = male, 4 = 4 kmlh level, 8 = 8 kmlh level

Downloaded from SAE International by John Schmidt, Tuesday, November 10, 2015

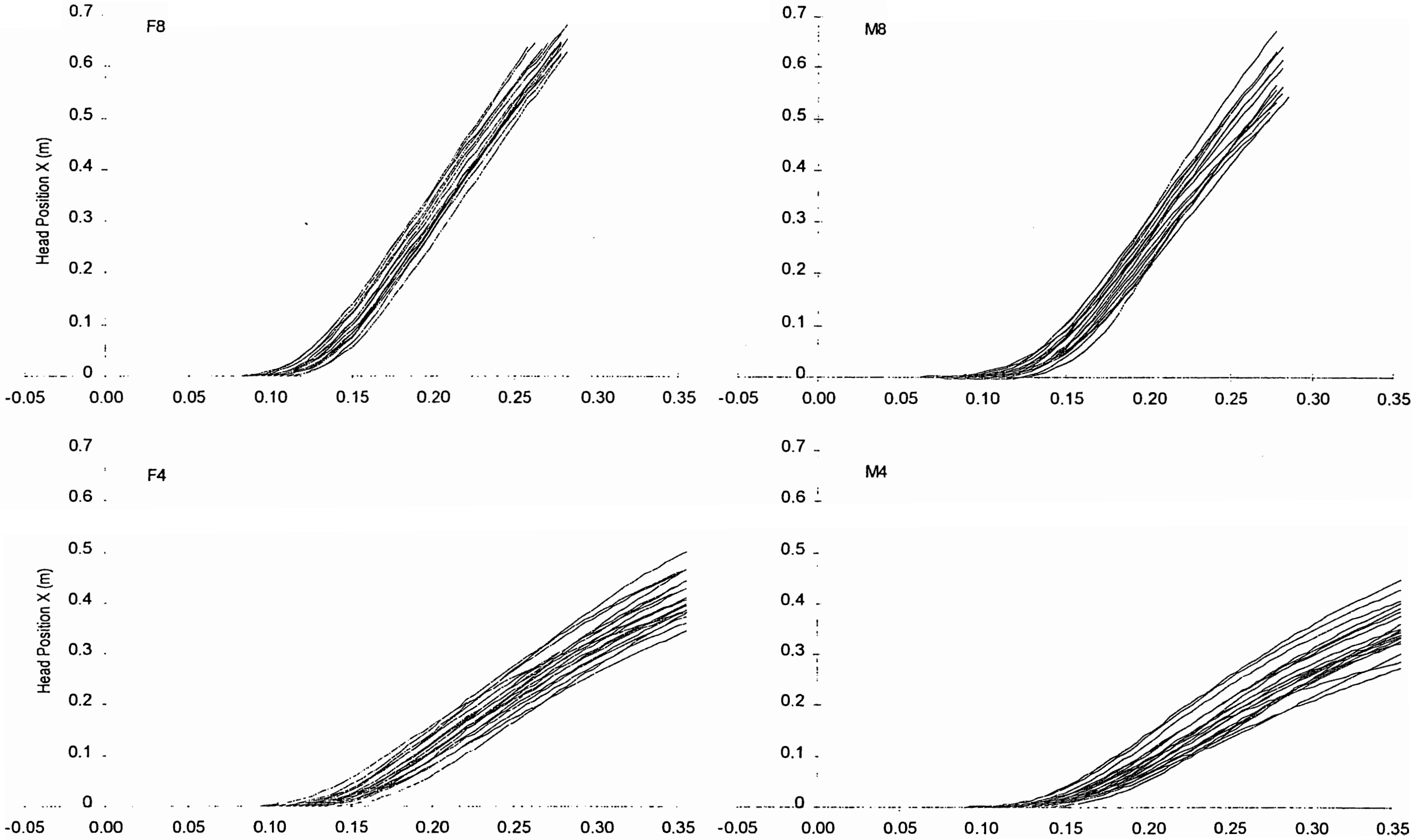

Figure A5. Head position (m) in the x-direction as a function of time (s). F = female, M = male, 4 = 4 km/h level, 8 = 8 kmlh level

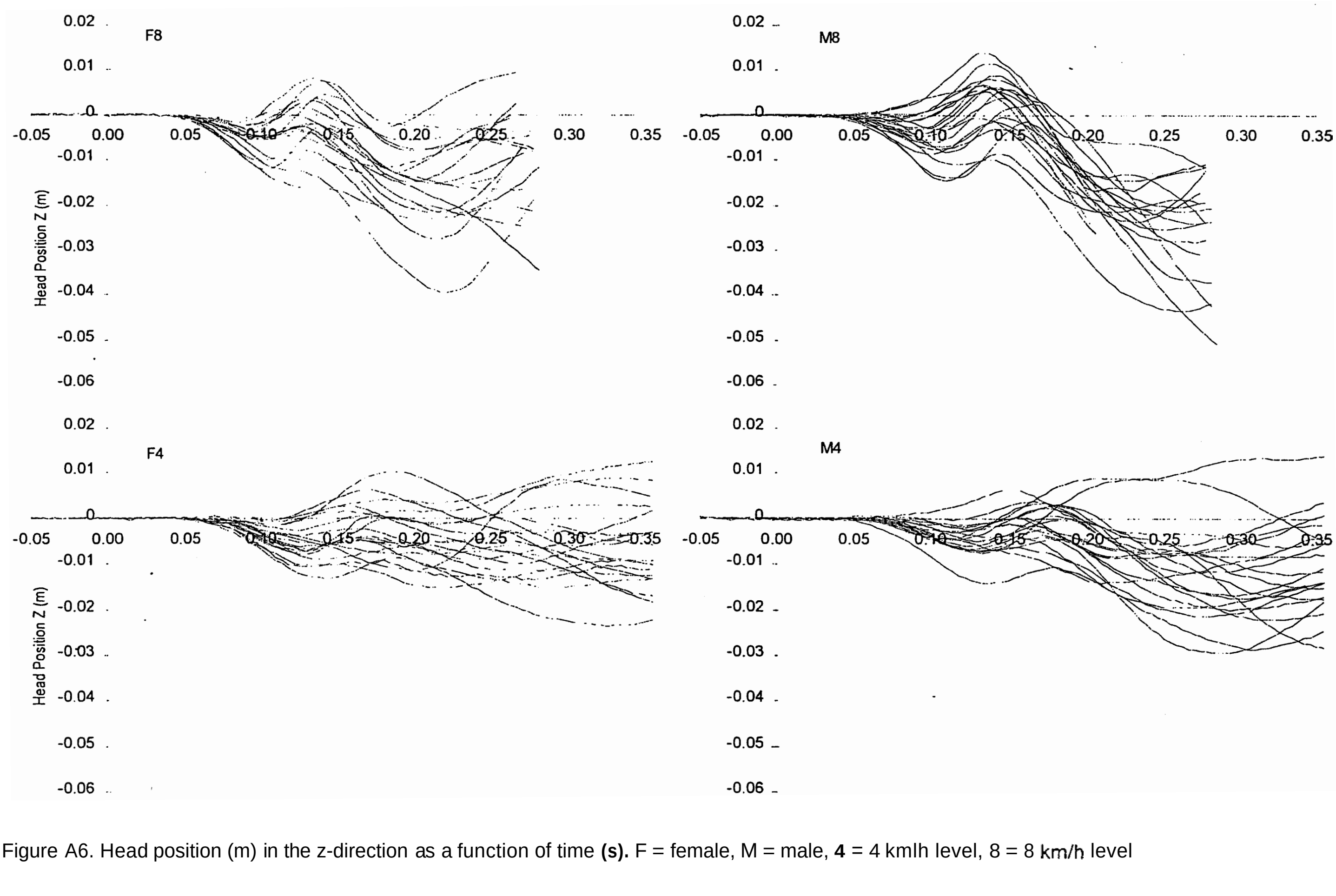

Figure A6. Head position (m) in the z-direction as a function of time **(s).** F = female, M = male, **4** = 4 kmlh level, 8 = 8 km/h level

Downloaded from SAE International by John Schmidt, Tuesday, November 10, 2015

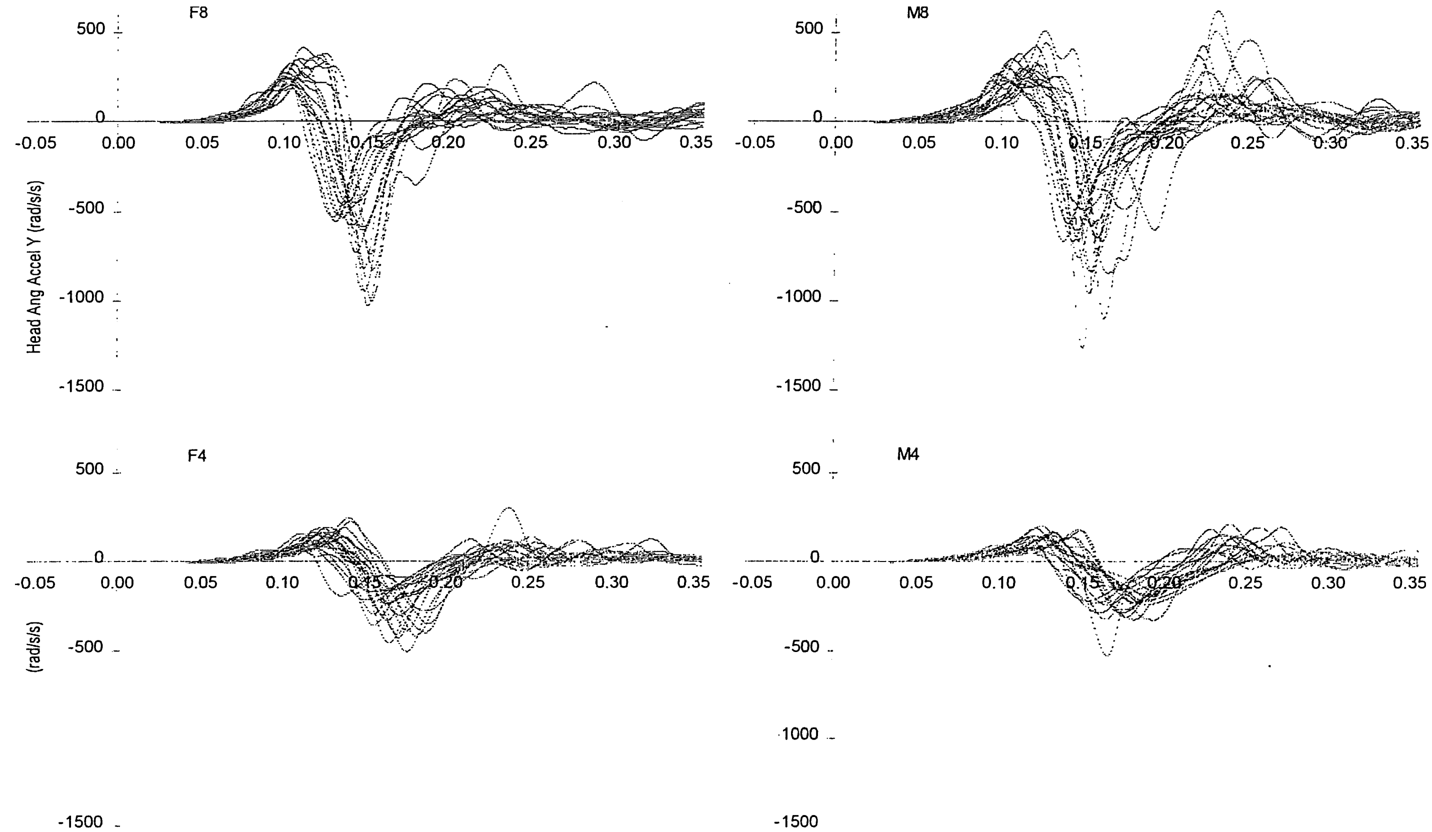

Figure A7. Head angular acceleration (radls^2) about the y-axis as a function of time (s). F = female, M = male, **4** = 4 kmlh level, 8 = 8 kmlh level.

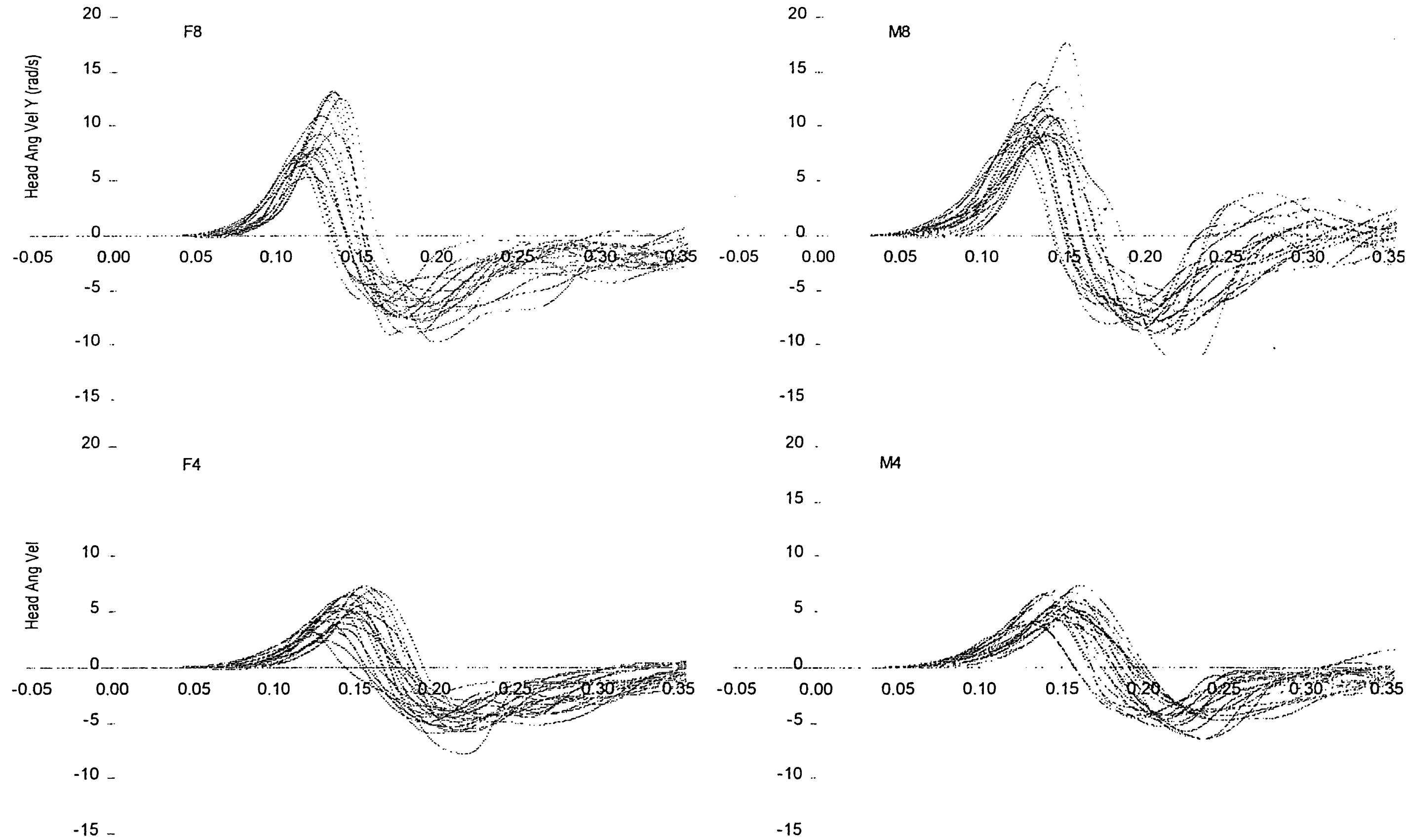

Figure A8. Head angular velocity (radls) about the y-axis as a function of time (s). F =female, M = male, **4 = 4** kmlh level, 8 = 8 kmlh level.

Downloaded from SAE International by John Schmidt, Tuesday, November 10, 2015

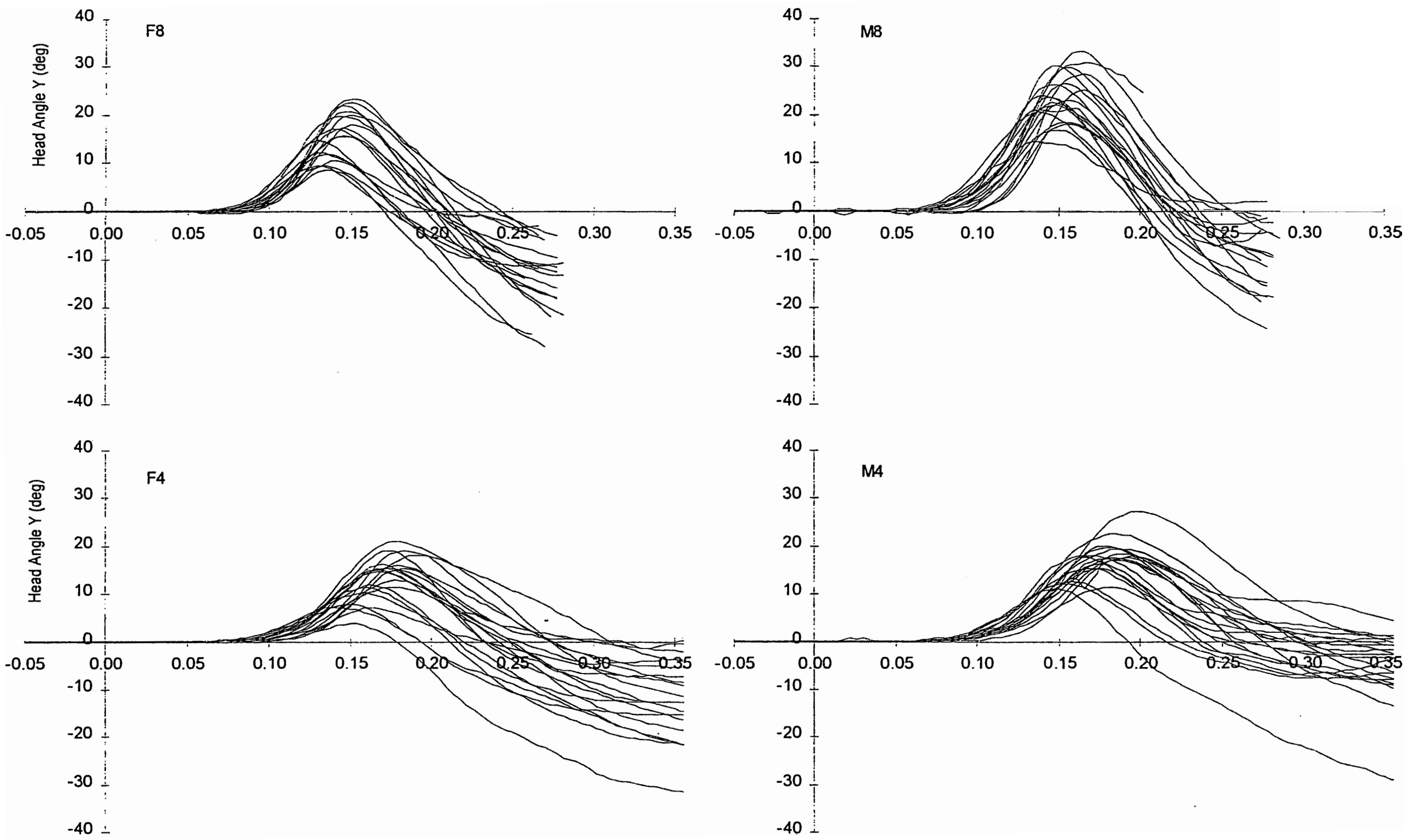

Figure A9. Head angle (degrees) about the y-axis as a function of time. Note that extension is positive and flexion is negative.

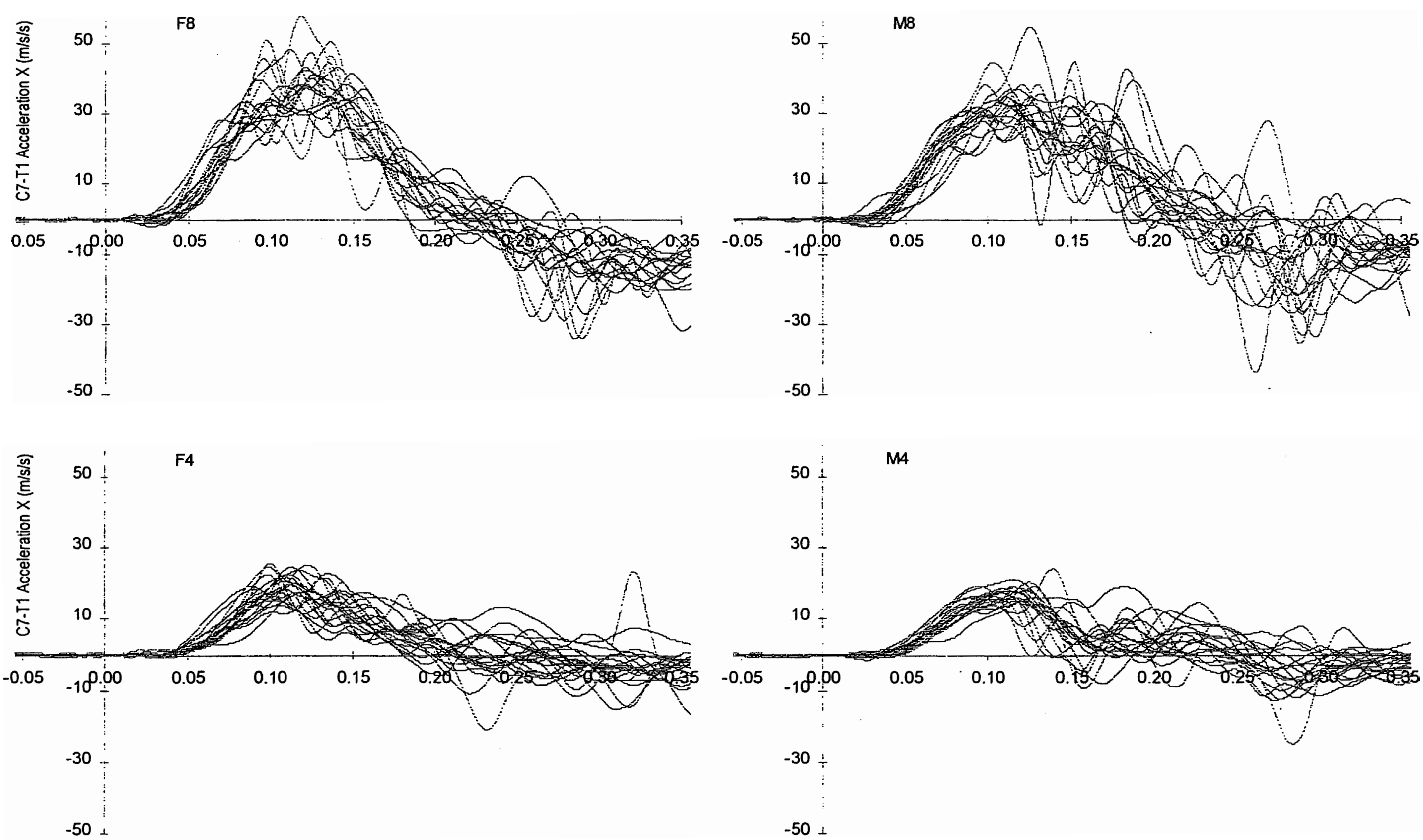

Figure A10. C7-T1 acceleration (m/s^2) in the x-direction as a function of time (s). F = female, M = male, 4 = 4 kmlh level, 8 = 8 km/h level

Downloaded from SAE International by John Schmidt, Tuesday, November 10, 2015

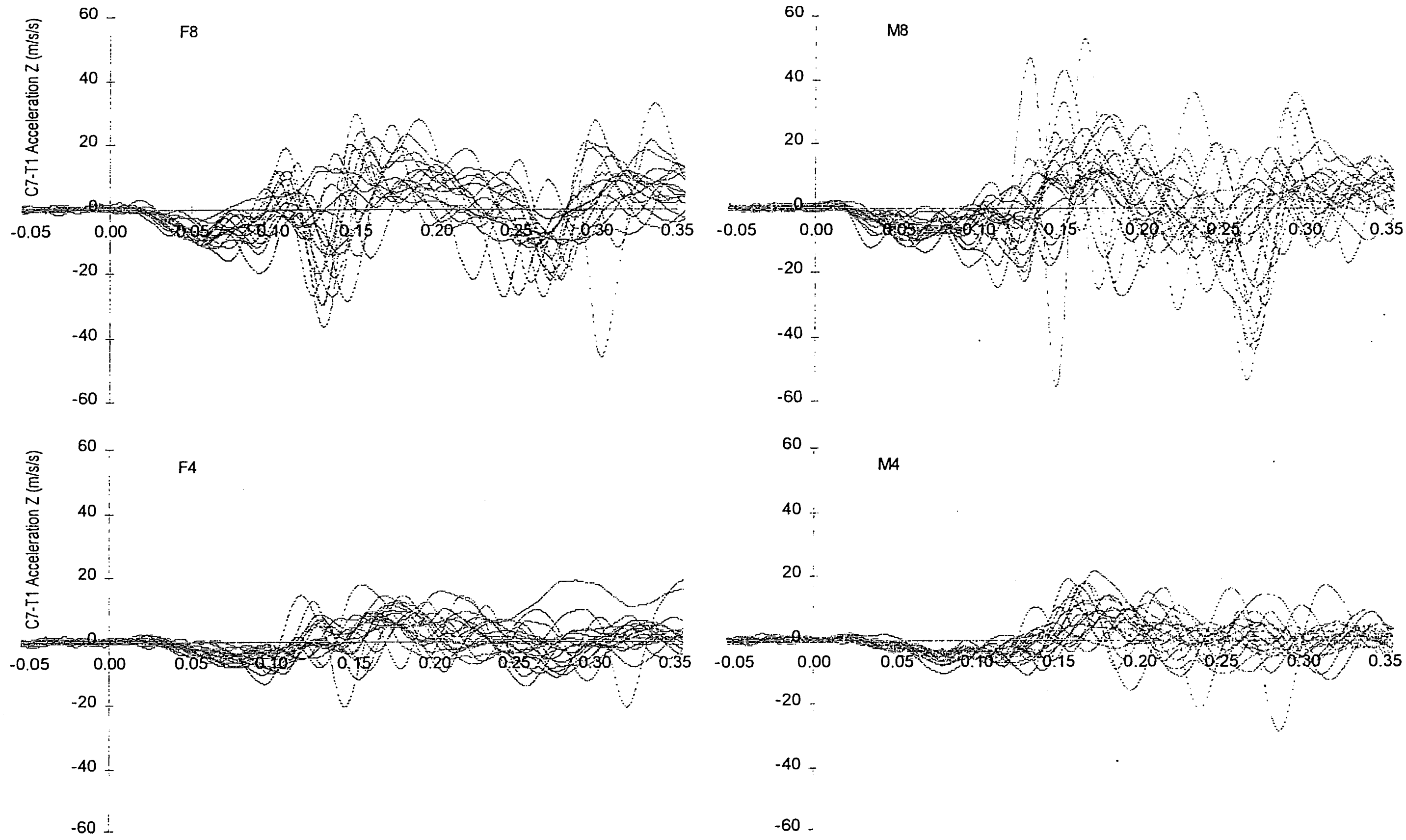

Figure A11. C7-T1 acceleration (m/s^2) in the z-direction as a function of time *(s)*. F = female, M = male, **4 =** 4 kmlh level, 8 = 8 kmlh level.

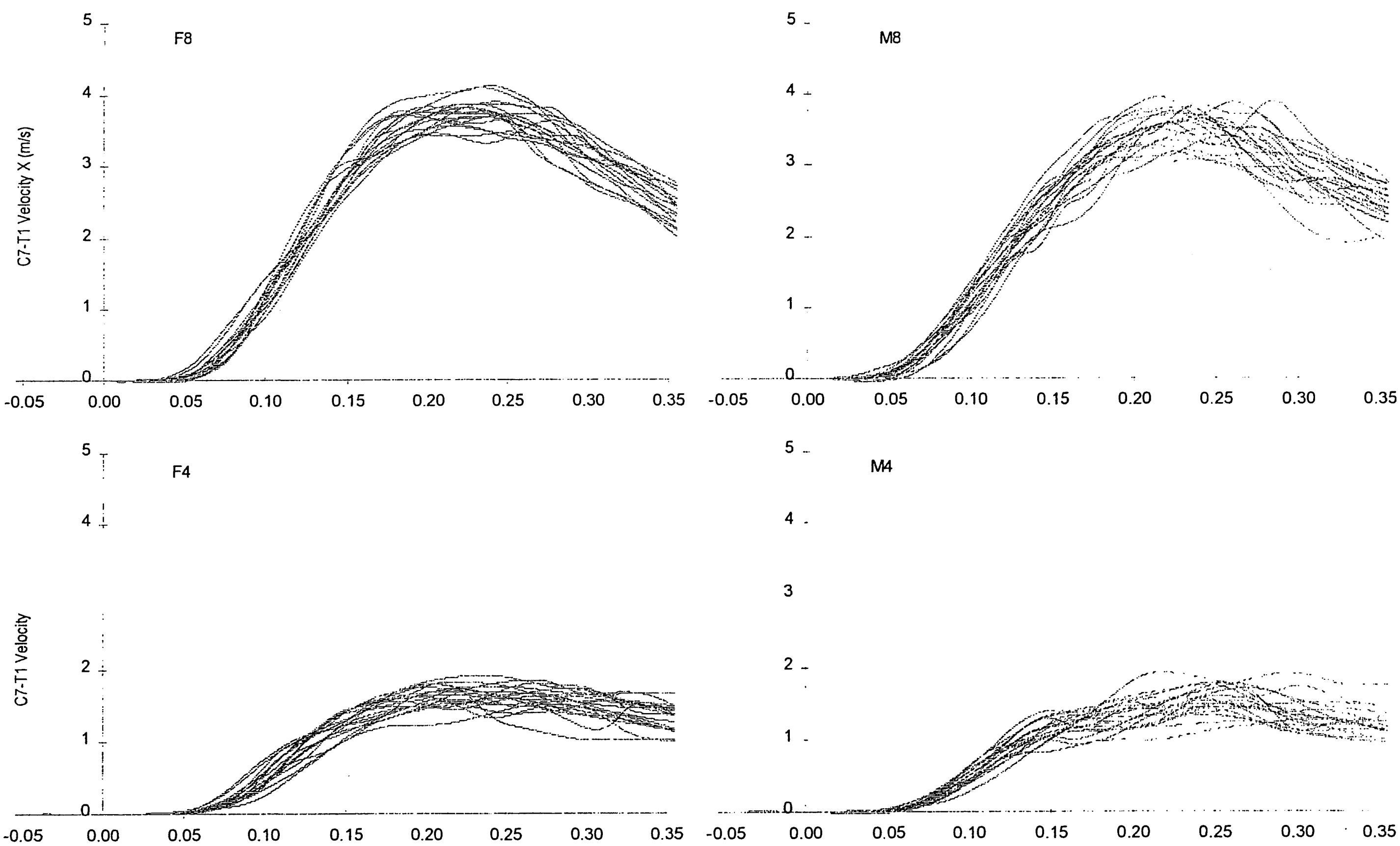

Figure A12. C7-T1 velocity (m/s) in the x-direction as a function of time (s). F =female, M = male, **4** = 4 kmlh level, 8 = 8 kmlh level.

Downloaded from SAE International by John Schmidt, Tuesday, November 10, 2015

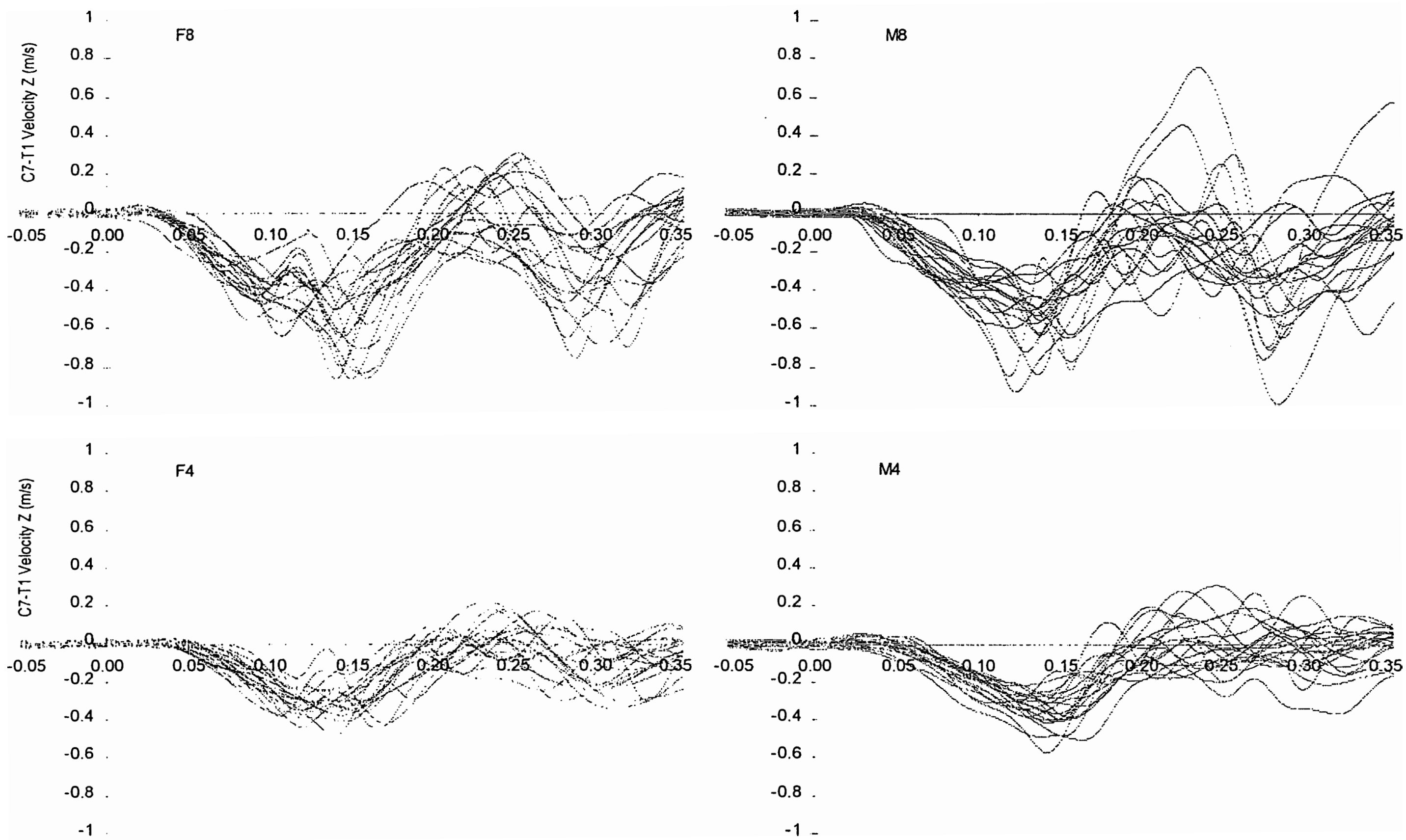

Figure A13. C7-T1 velocity (m/s) in the z-direction as a function of time (s). F = female, M = male, 4 = 4 km/h level. 8 = 8 kmlh level

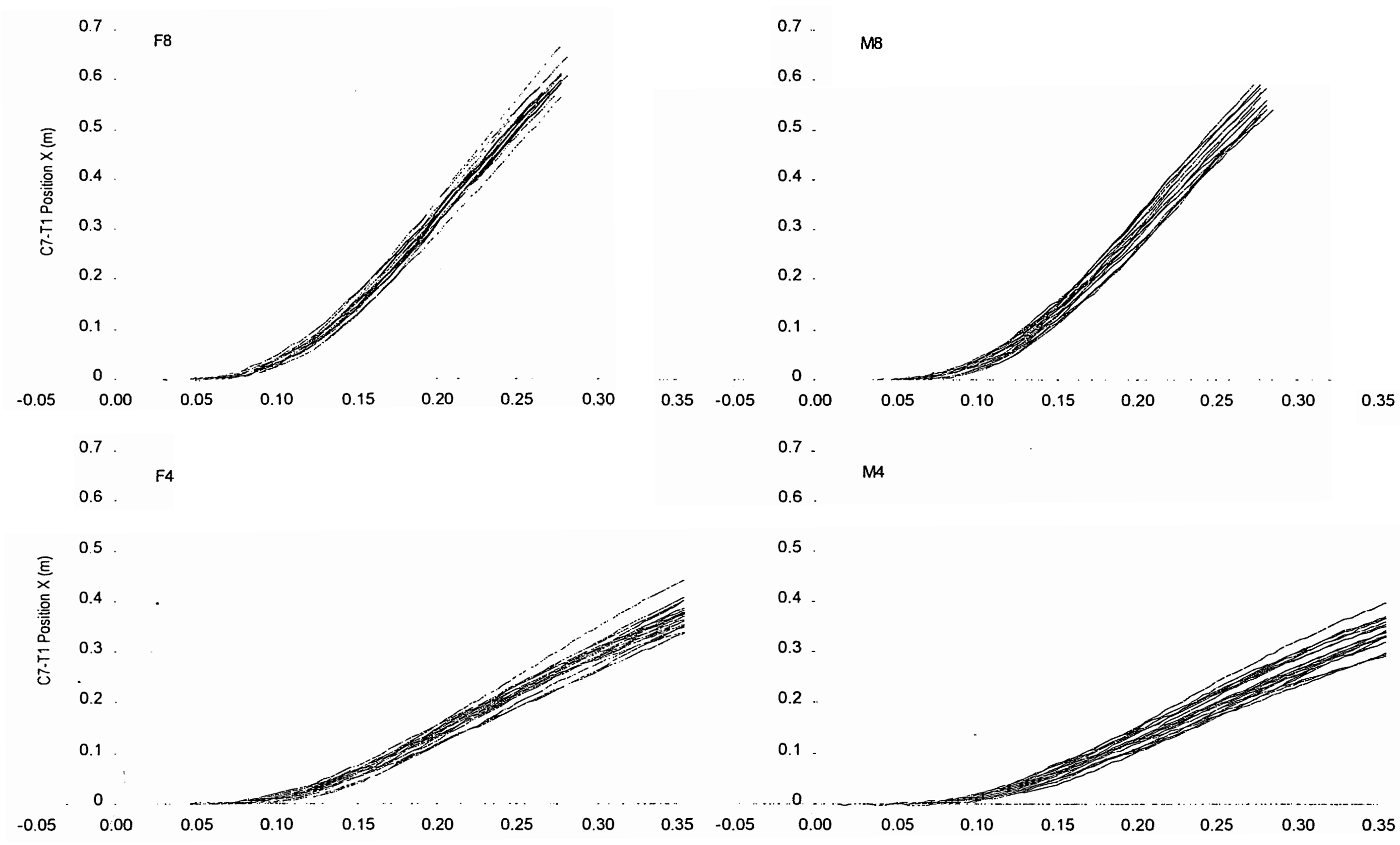

Figure A14. C7-T1 position (m) in the x-direction as a function of time (s). F = female, M = male, 4 = 4 kmlh level, 8 = 8 kmlh level.

Downloaded from SAE International by John Schmidt, Tuesday, November 10, 2015

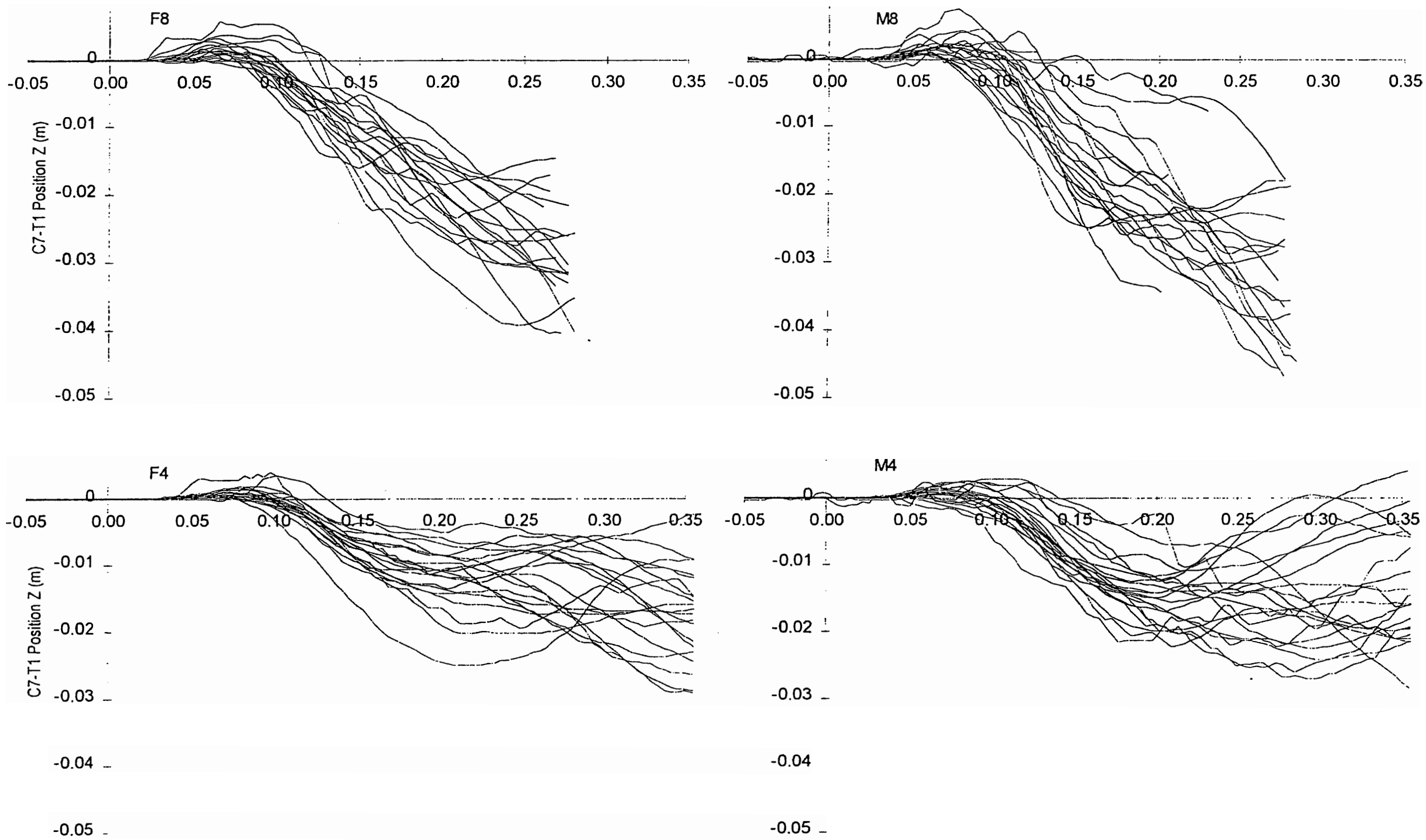

Figure A15. C7-T1 position (m) in the z-direction as a function of time (s). F = female, M = male, **4** = **4** km/h level, 8 = 8 kmlh level

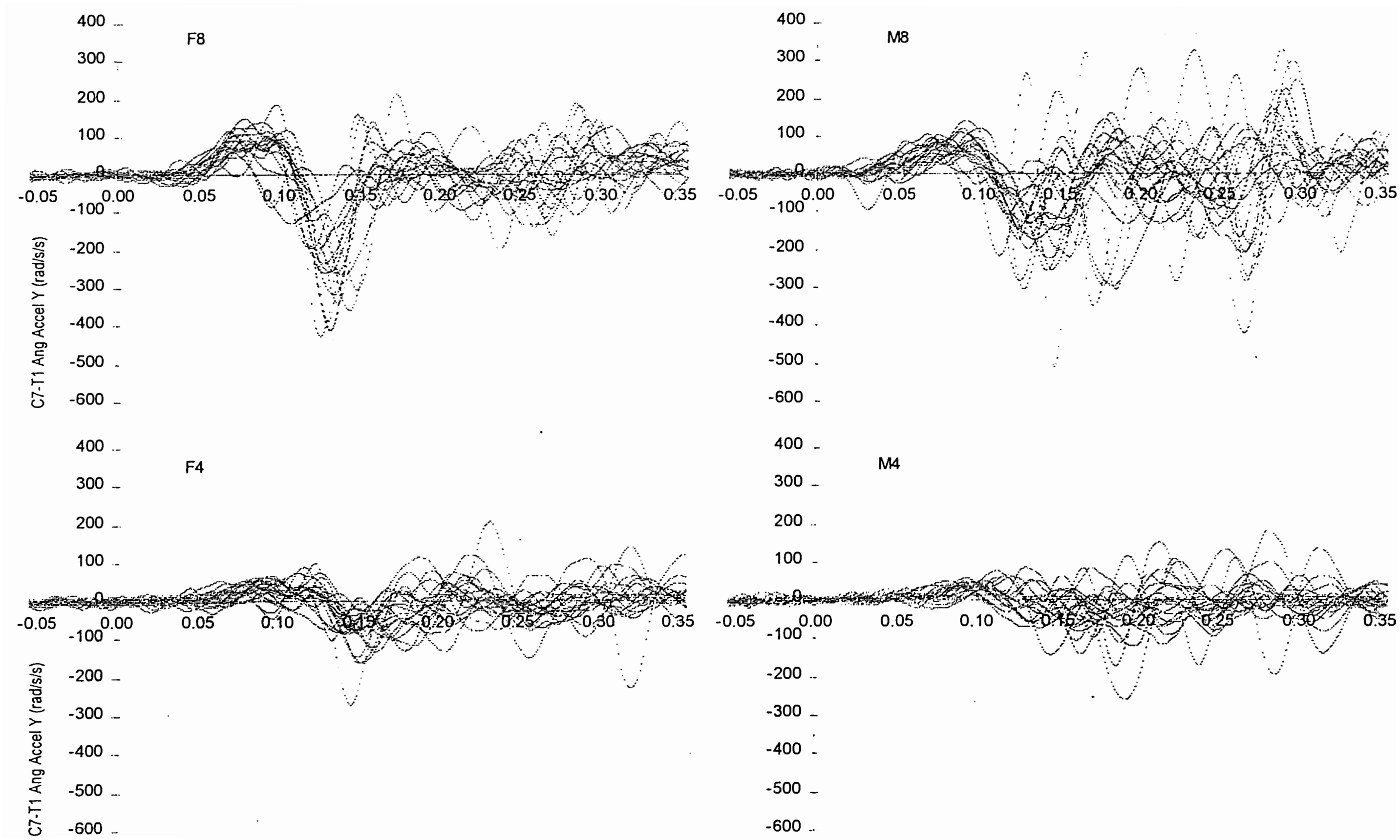

Figure A16. C7-T1 angular acceleration (rad/s^2) about the y-axis as a function of time (s). F = female, M = male, 4 = 4 kmlh level, 8 = 8 km/h level.

Downloaded from SAE International by John Schmidt, Tuesday, November 10, 2015

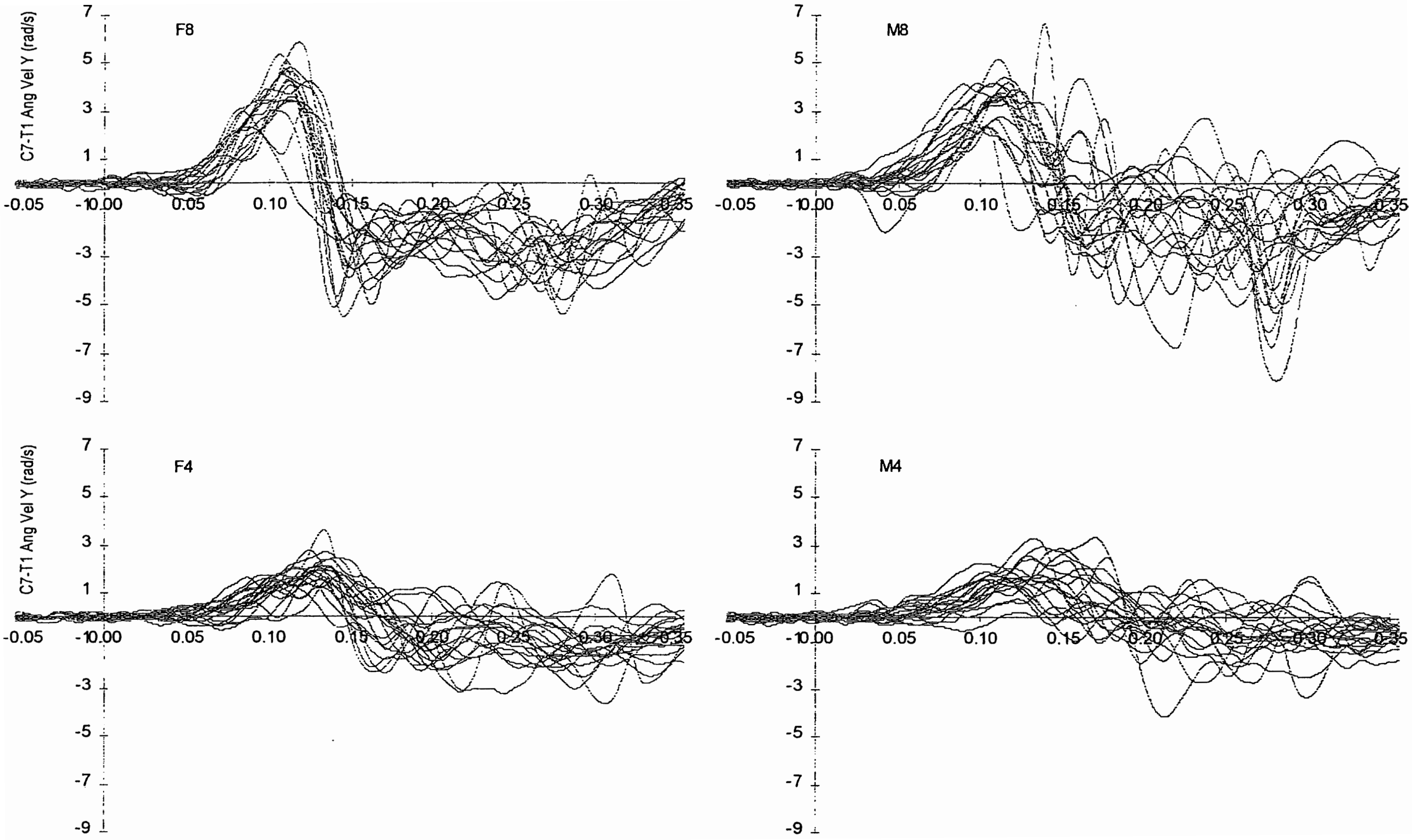

Figure A17. C7-T1 angular velocity (rad/s) about the y-axis as a function of time (s). F = female, M = male, 4 = 4 kmlh level, 8 = 8 kmlh level.

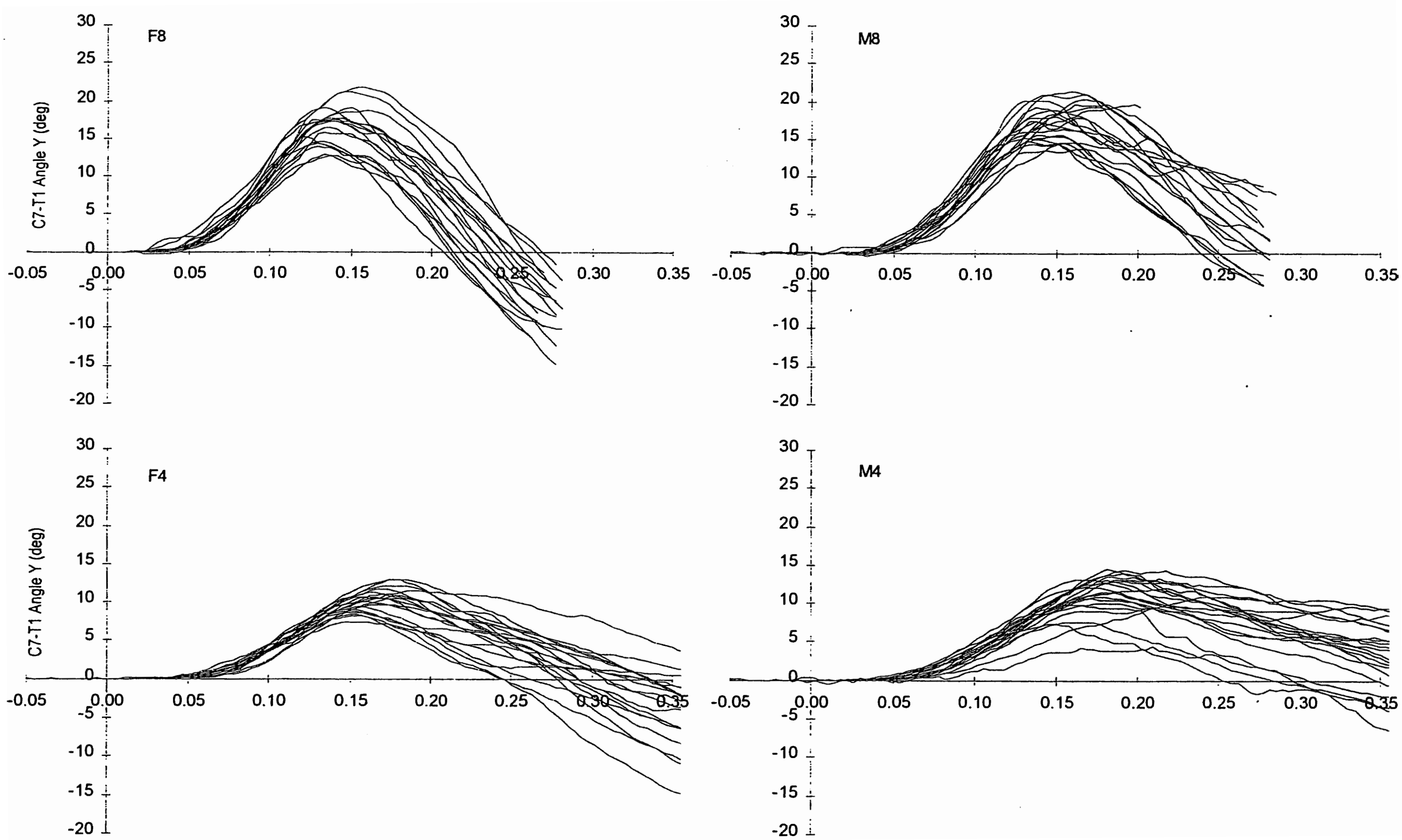

Figure A18. C7-T1 angle (deg) about the y-axis as a function of time (s). Note that extension is positive and flexion is negative

Downloaded from SAE International by John Schmidt, Tuesday, November 10, 2015

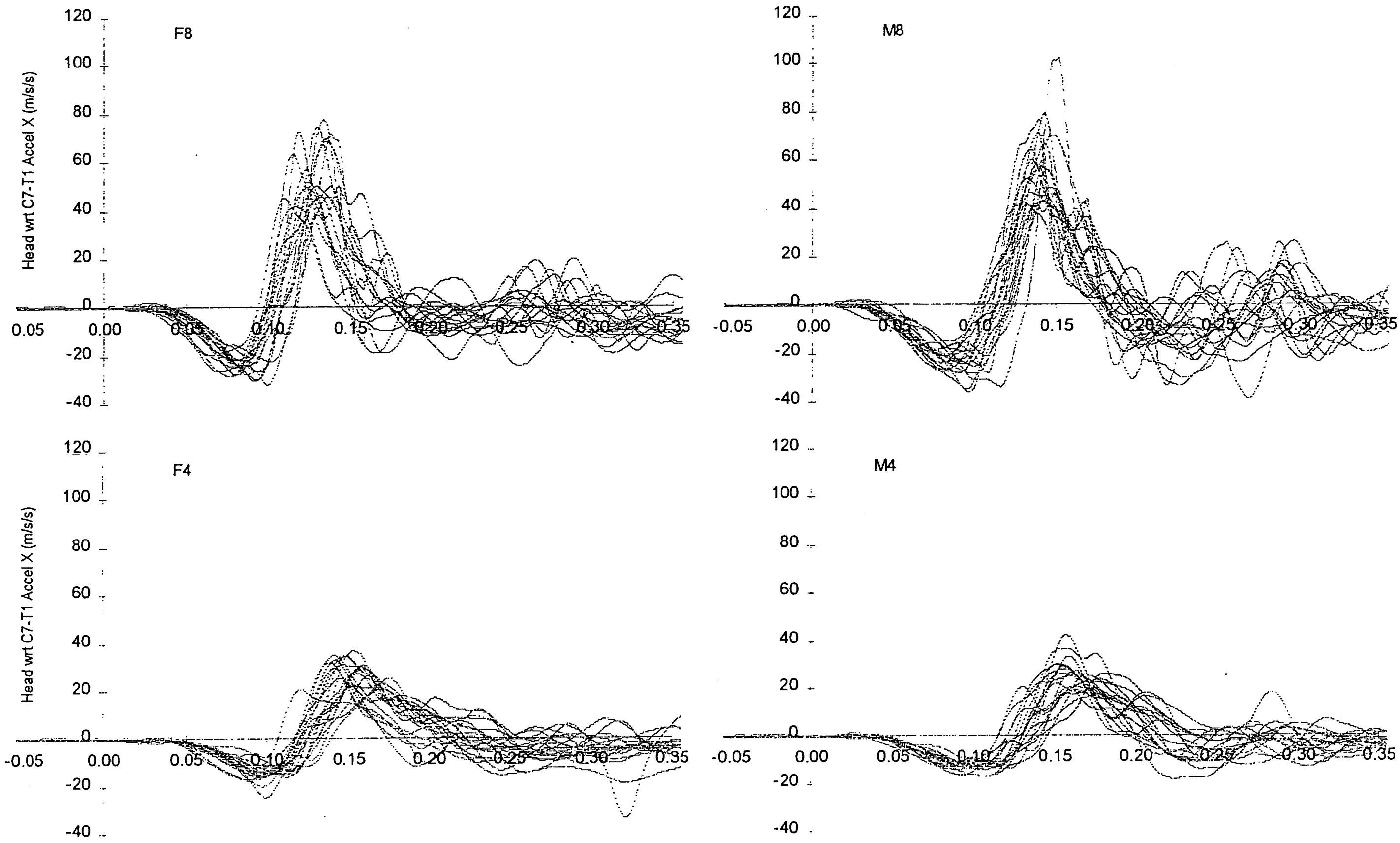

Figure A19. Head acceleration (m/s^2) with respect to C7-T1 in the x-direction as a function of time (s). F = female, M = male, 4 = 4 kmlh, 8 = 8 km/h

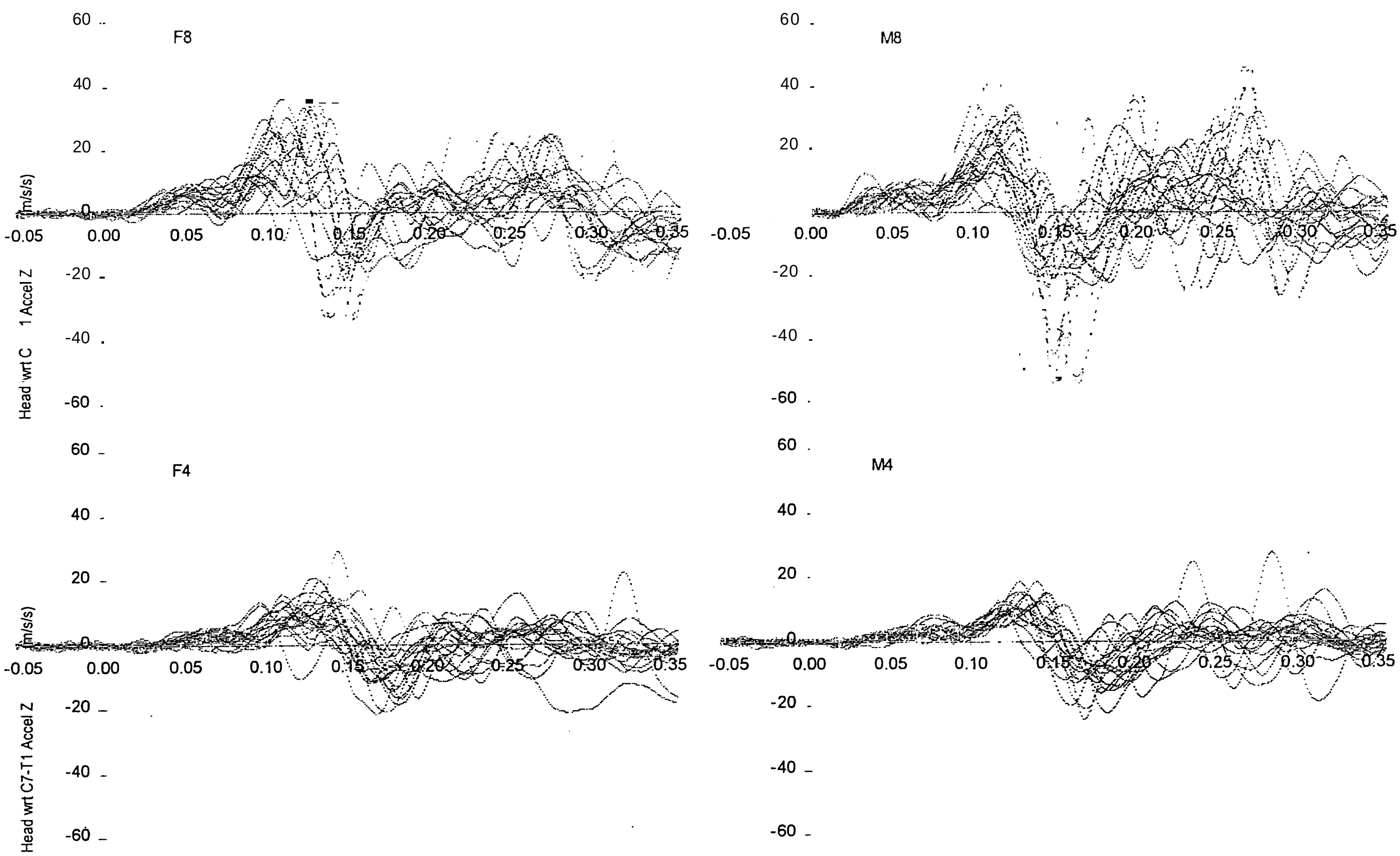

Figure A20. Head acceleration (mls^2) with respect to C7-T1 in the z-direction as a function of time (s). F = female, M = male, 4 = 4 kmlh, 8 = 8 kmlh

Downloaded from SAE International by John Schmidt, Tuesday, November 10, 2015

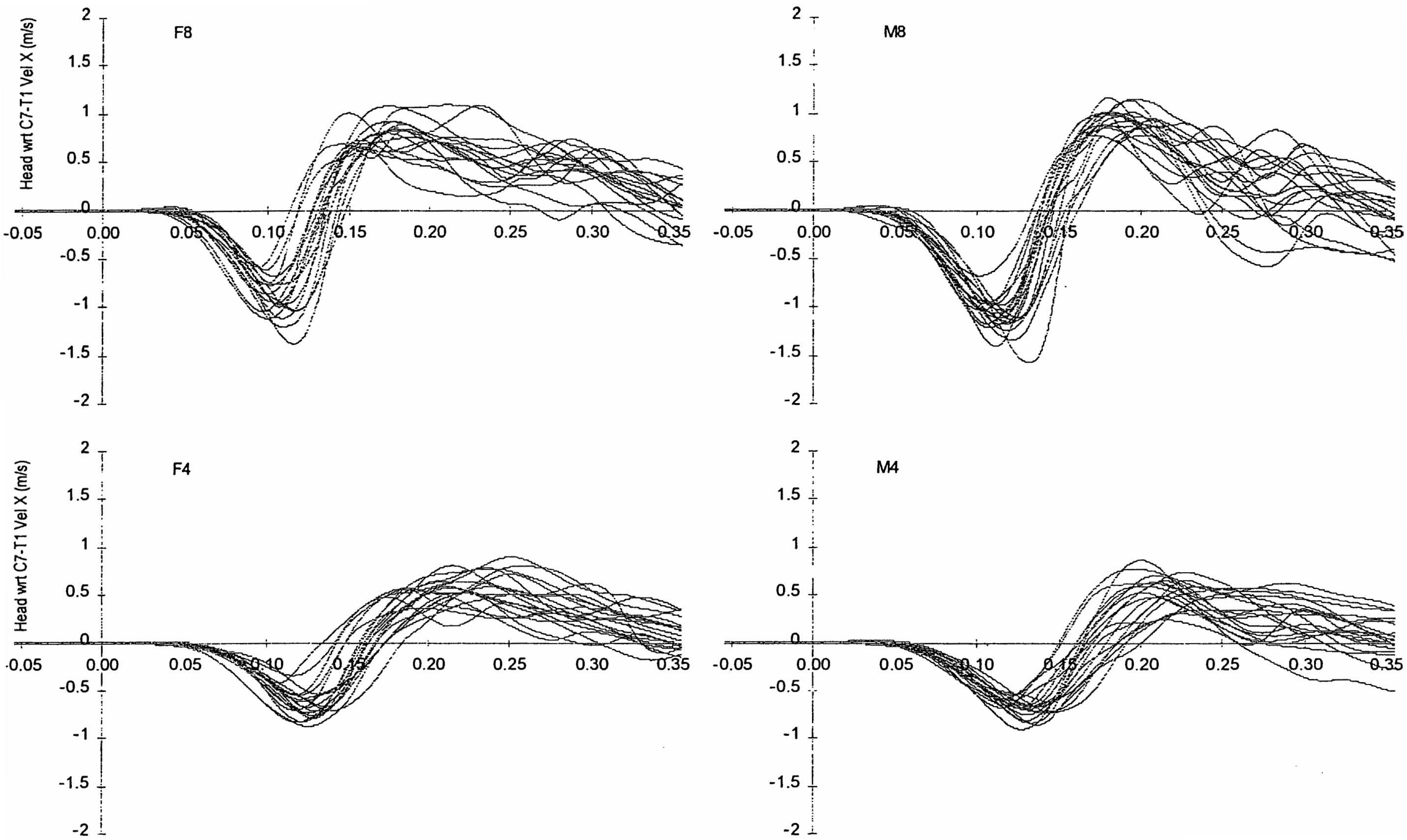

Figure A21. Head velocity (mls) with respect to C7-T1 in the x-direction as afunction of time (s). F = female, M = male, **4** = **4** kmlh, 8 = 8 kmlh.

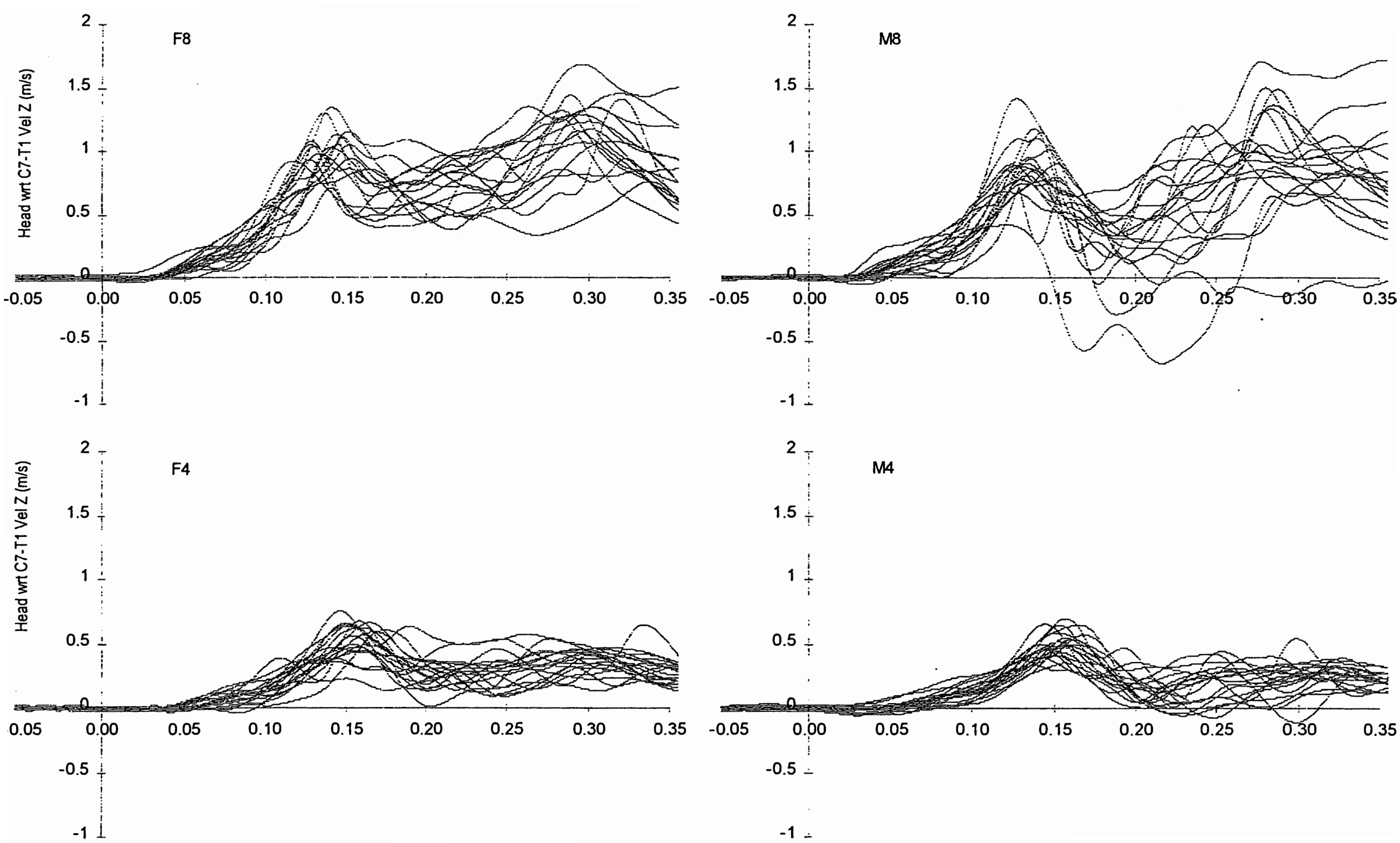

Figure A22. Head velocity (m/s) with respect to C7-T1 in the z-direction as **a** function of time (s). F = female, M = male, **4** = **4** kmlh, 8 = 8 kmlh.

Downloaded from SAE International by John Schmidt, Tuesday, November 10, 2015

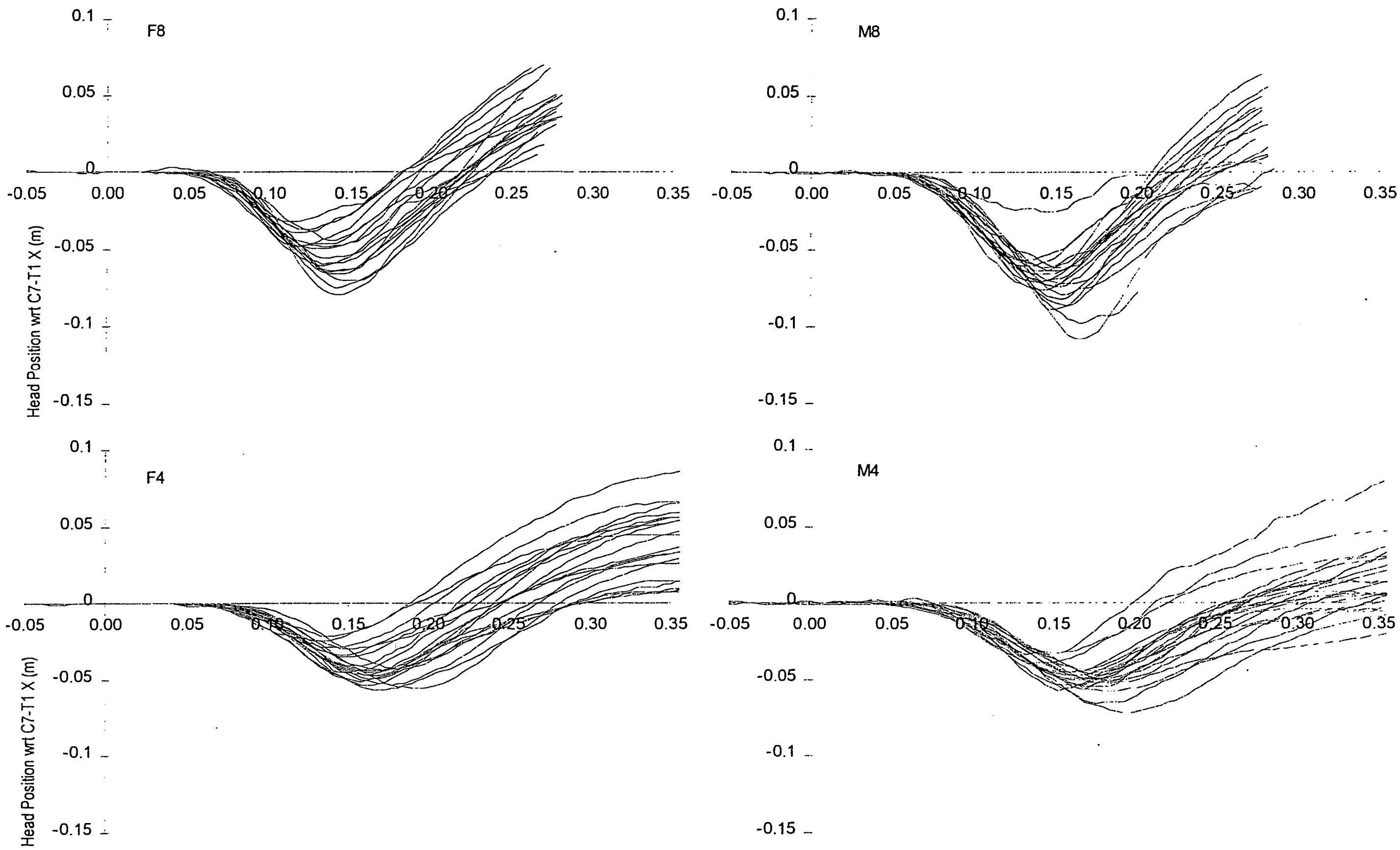

Figure A23. Head position (m) with respect to C7-T1 in the x-direction as a function of time (s). F = female, M = male, 4 = 4 km/h, 8 = 8 km/h

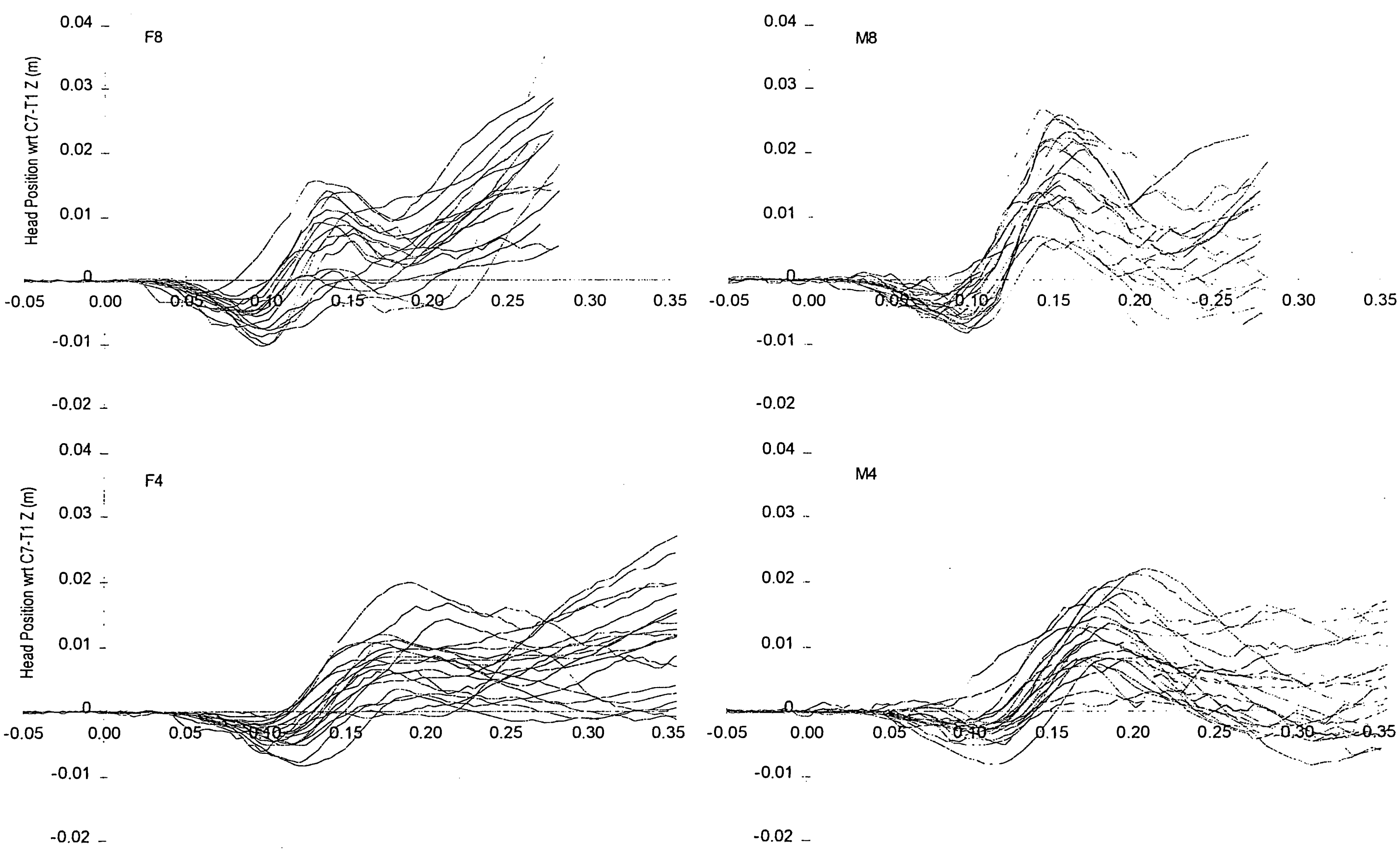

Figure A24. Head position (m) with respect to C7-T1 in the z-direction as a function of time (s). F = female, M = male, **4** = 4 km/h, 8 = 8 km/h

Downloaded from SAE International by John Schmidt, Tuesday, November 10, 2015

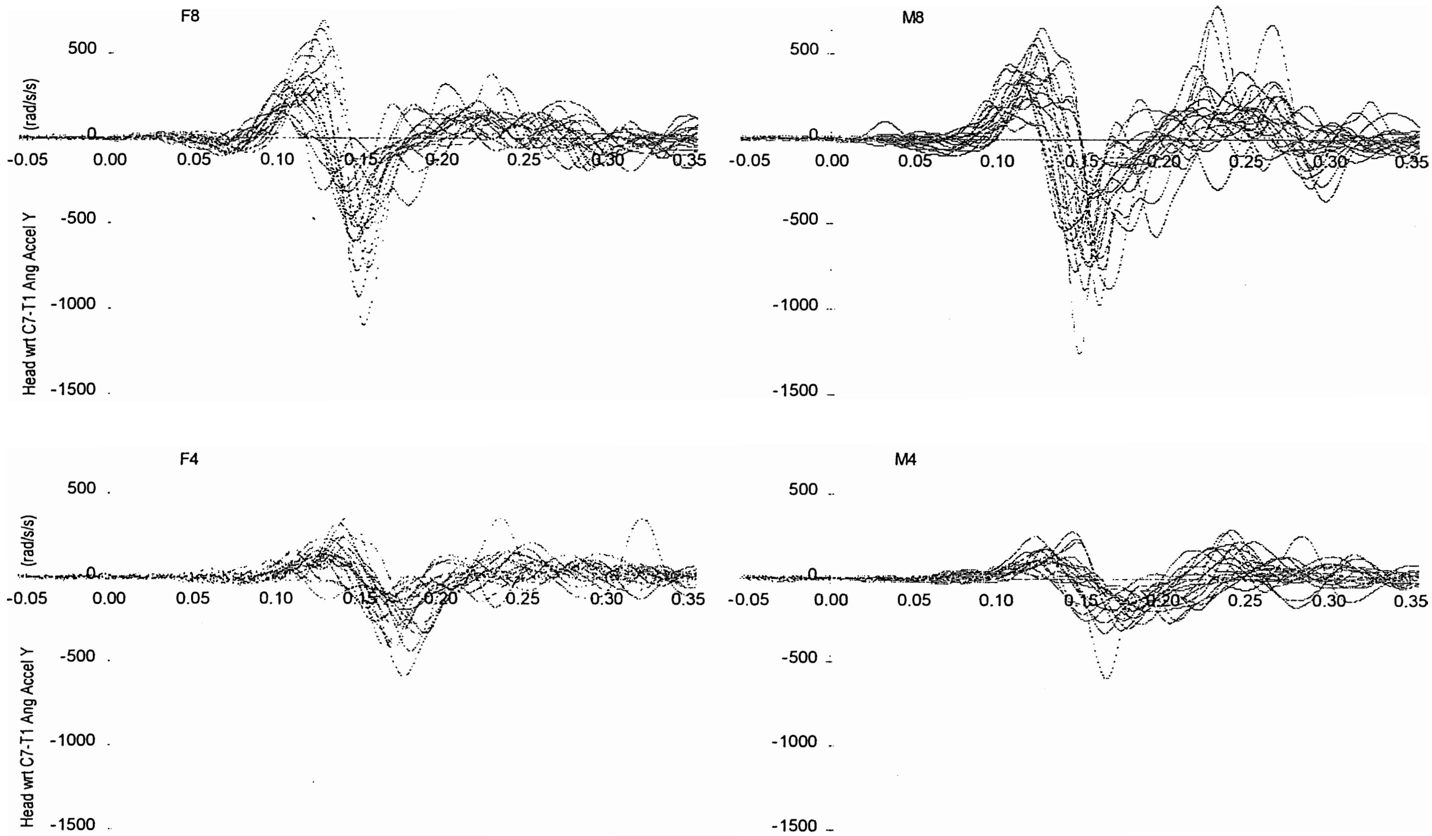

Figure **A25.** Head angular acceleration (rad/s^2) with respect to C7-T1 about the y-axis as a function of time (s). F = female, M = male, **4 = 4** km/h, 8 = 8 km/h.

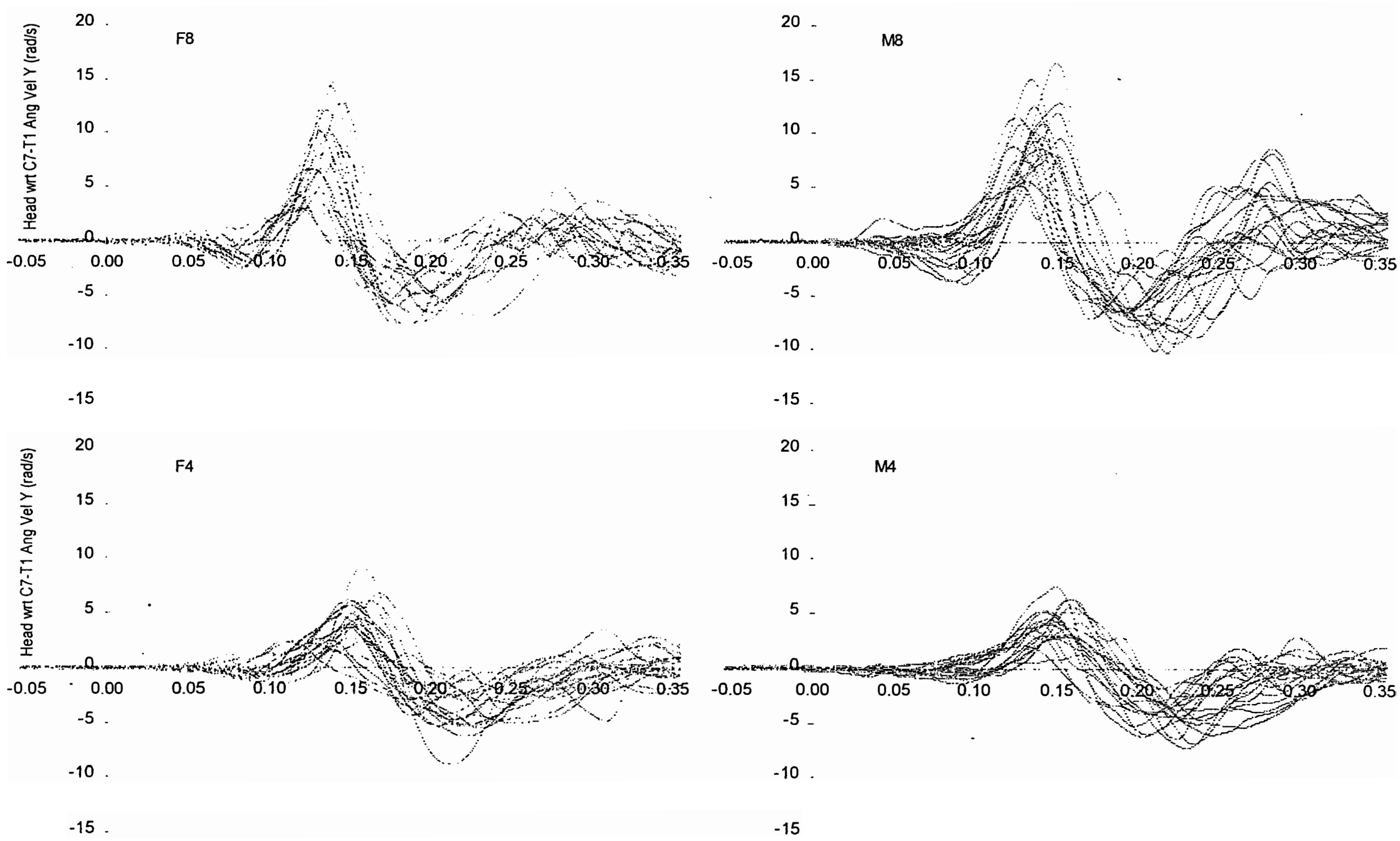

Figure A26. Head angular velocity (rad/s) with respect to C7-T1 in the x-direction as a function of time **(s).** F = female, M = male, **4 = 4** km/h, 8 = 8 kmlh.

Downloaded from SAE International by John Schmidt, Tuesday, November 10, 2015

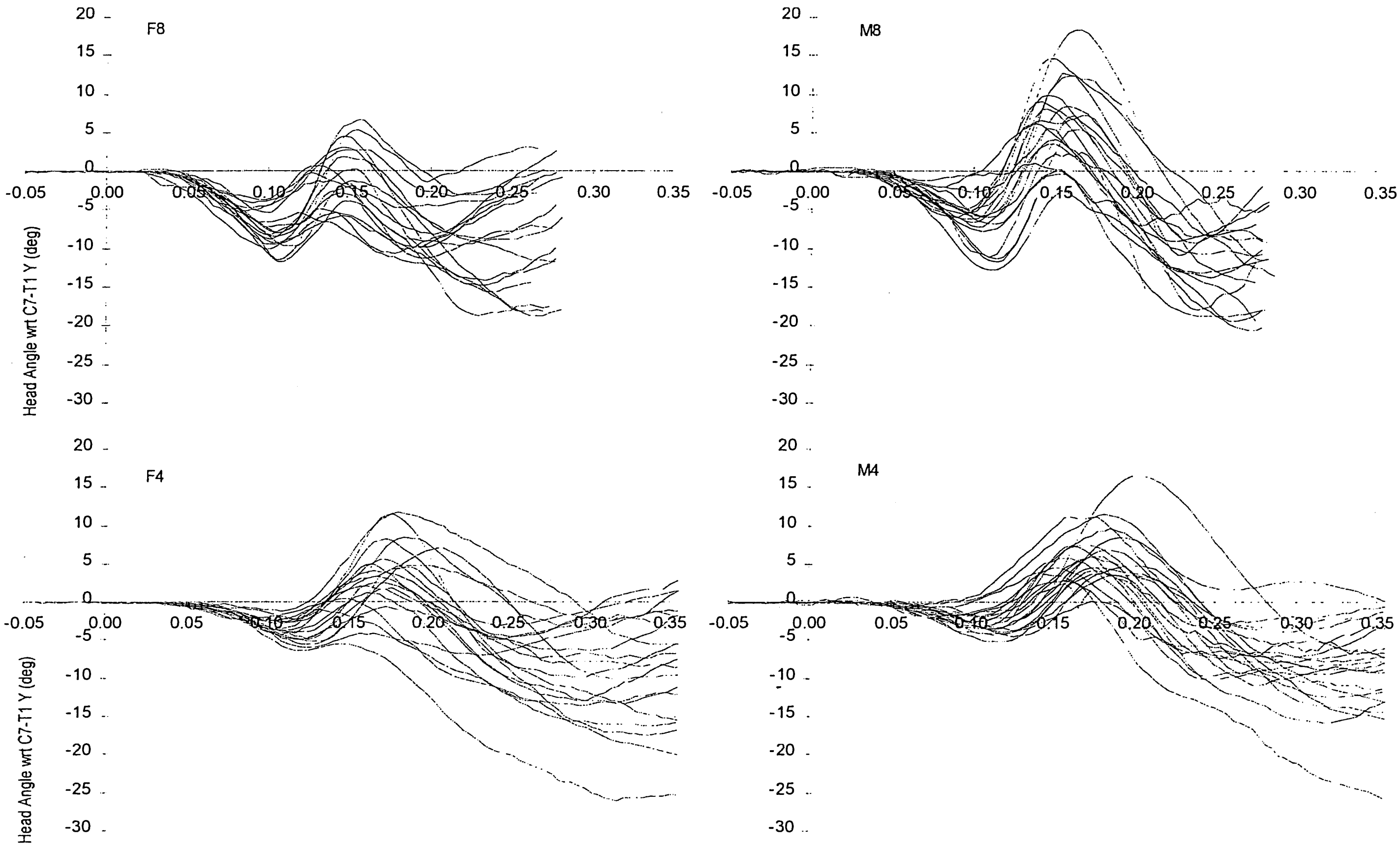

Figure A27. Head angle (deg) with respect to C7-T1 about the y-axis as a function of time (s). Note that extension is positive and flexion is negative